

1 **Bayesian network modelling of phosphorus pollution in agricultural catchments**  
2 **with high-resolution data**

3 *Authors:* Negri C.<sup>1,2,3,4</sup> (0000-0001-8917-5322), Mellander P-E. <sup>1</sup> (0000-0002-7261-  
4 6758), Schurch N.J.<sup>4</sup> (0000-0001-9068-9654), Wade A. J. <sup>3</sup> (0000-0002-5296-8350),  
5 Zisis Gagkas<sup>2</sup> (0000-0002-9477-4407), Douglas H. Wardell-Johnson<sup>2</sup> (0000-0003-  
6 4979-0202), Kerr Adams<sup>2</sup> (0000-0002-0049-9871), Glendell M.<sup>2</sup> (0000-0003-0110-  
7 9879)

8 *Authors' Affiliations:* <sup>1</sup>Agricultural Catchments Programme, Teagasc Environment  
9 Research Centre, Johnstown Castle, Co. Wexford Y35 Y521, <sup>2</sup>The James Hutton  
10 Institute, Craigiebuckler, Aberdeen AB15 8QH, <sup>3</sup>University of Reading, School of  
11 Archaeology, Geography and Environmental Science, Whiteknights, Reading, RG6  
12 6AB, <sup>4</sup>Biomathematics and Statistics Scotland, Craigiebuckler, Aberdeen AB15 8QH.

13 *Corresponding Author:* Camilla Negri, email: [camilla.negri@hutton.ac.uk](mailto:camilla.negri@hutton.ac.uk), address:  
14 The James Hutton Institute, Craigiebuckler, Aberdeen AB15 8QH, Scotland UK

15  
16  
17  
18  
19  
20  
21  
22

23 This is a non-peer reviewed pre-print submitted to EarthArXiv. It has been submitted to  
24 Environmental Modelling & Software for peer review.

## 25 **Abstract:**

26 A Bayesian Belief Network was developed to simulate phosphorus (P) loss in an Irish  
27 agricultural catchment. Septic tanks and farmyards were included to represent all P sources and  
28 assess their effect on model performance. Bayesian priors were defined using daily discharge  
29 and turbidity, high-resolution soil P data, expert opinion, and literature. Calibration was done  
30 against seven years of daily Total Reactive P concentrations. Model performance was  
31 assessed using percentage bias, summary statistics, and visually comparing distributions. Bias  
32 was within acceptable ranges, the model predicted mean and median P concentrations within  
33 the data error, with simulated distributions wider than the observations. Considering the risk of  
34 exceeding regulatory standards, predictions showed lower P losses than observations, likely  
35 due to simulated distributions being left-skewed. We discuss model advantages and  
36 limitations, the benefits of explicitly representing uncertainty, and priorities for data collection  
37 to fill knowledge gaps present even in a highly monitored catchment.

38 **Keywords:** diffuse pollution; point sources; high-resolution water-quality monitoring;  
39 participatory model; uncertainty analysis

## 40 **Highlights:**

41

- 42 • First study evaluating Bayesian Network of P pollution against high-resolution data
- 43 • Bayesian model allowed knowledge gap identification in a highly monitored catchment
- 44 • Model shows strong predictive performance against the observed interquartile ranges
- 45 • Model structural, data and parametric uncertainties are represented
- 46 • Wide posterior distributions are an inherent property of the modelling approach

## 47 **1. Introduction**

48 Phosphorus (P) losses from farmland to surface waters (diffuse P losses) continue to be a major  
49 cause of water quality deterioration and eutrophication (European Environment Agency, 2019).

50 P remains a major source of water quality failures in Ireland, particularly due to the slow release  
51 of soil legacy P (Schulte et al., 2010), which is often unaccounted for in soil P tests (Thomas  
52 et al., 2016b). There are multiple challenges facing land managers, stakeholders, and  
53 policymakers when tackling P pollution in agricultural catchments in Northwest Europe (Bol  
54 et al., 2018). Smaller catchments (<50 km<sup>2</sup>) vary in their vulnerability to P losses, necessitating  
55 a catchment-specific understanding of stressor-impact relationships and targeting of mitigation  
56 measures (Glendell et al., 2019). Drivers of P transfer differ across spatial scales (point, plot,  
57 field, hillslope, and catchment), and the understanding gained from laboratory or field  
58 measurements may not be directly applicable at the catchment scales represented in models  
59 (Brazier et al., 2005; Wade et al., 2008). Additionally, the understanding of key drivers of  
60 catchment vulnerability is complicated by different P sources and pathways that result in  
61 similar concentration-discharge hysteresis relationships at the catchment outlet. This  
62 confounding often makes it difficult to determine the most important P sources and pathways  
63 to target with P reduction measures and to predict their likely effect (Bol et al., 2018).

64 Soil P content and excess plant available P, derived from fertilizer application, have been  
65 identified as the main sources of diffuse P in Irish agricultural catchments (Regan et al., 2012),  
66 while some studies stress the importance of point pollution sources (Campbell et al., 2015; Gill  
67 and Mockler, 2016; Vero et al., 2019) as well as legacy P (Thomas et al., 2016b). In addition,  
68 the transport and delivery of P in Irish agricultural catchments are dominated by weather and  
69 hydrological conditions rather than initial soil P (Mellander et al., 2018, 2015). To investigate  
70 diffuse P pollution sources in Irish agricultural catchments, modelers have used two main  
71 approaches: 1) the critical source areas (CSAs) approach (Packham et al., 2020; Thomas et al.,  
72 2016b, 2021), and 2) the load apportionment approach (Crockford et al., 2017; Mockler et al.,  
73 2017). CSAs methods aim at identifying and mapping areas of high hydrological activity  
74 connected with areas of elevated P mobilization, thus facilitating the transfer of P from

75 terrestrial to aquatic ecosystems (Djodjic and Markensten, 2019). One of the biggest  
76 advantages of CSAs is that they provide the basis to spatially identify potential locations for  
77 mitigation measures, however, these approaches require extensive sampling and mapping of P  
78 sources and hydrological connectivity, and provide qualitative results that might be difficult to  
79 interpret for policy, to validate, or evaluate at larger scales (Djodjic and Markensten, 2019). In  
80 contrast, Load Apportionment Models (LAMs), calculate nutrient loads from all sources and  
81 then estimate factors to reduce such loads to account for treatment (e.g. wastewaters) or  
82 environmental attenuations. Estimated loads are then compared with loads calculated from  
83 measurements (Mockler et al., 2016). This method can identify the dominant pollution  
84 contributors in catchments and sub-catchments, while also assessing management strategies  
85 (Mockler et al., 2016). However, LAMs can be difficult to interpret for non-experts, because  
86 of the uncertainties around load estimation, especially when used with low-frequency datasets,  
87 which limits their utility as management tools (Crockford et al., 2017).

88 Catchment nutrient models are crucial to summarize current knowledge and process  
89 understanding, as well as to test land use and climate scenario effects on water quality, which  
90 can inform mitigation action (Jackson-Blake et al., 2015). However, mechanistic models of  
91 water quality (e.g. catchment scale P models like INCA-P, (Jackson-Blake et al., 2016)), can  
92 have parameters that are unmeasurable yet heavily influence model outputs (Jackson-Blake et  
93 al., 2017) and are often over-parameterized, especially when upscaling to watershed scales  
94 (Radcliffe et al., 2009). Additionally, P models often perform inadequately in rural catchments  
95 where diffuse sources are dominant, and model outputs' accuracy is limited by current  
96 knowledge (Jackson-Blake et al., 2015). Furthermore, water quality and nutrient transport  
97 models are frequently hindered by constraints associated with available data, the presence of  
98 non-linear interactions, and temporal and spatial scale representation issues (Blöschl et al.,  
99 2019; Harris and Heathwaite, 2012; Rode et al., 2010; Wellen et al., 2015). Hence, there is a

100 recognition of the importance of incorporating uncertainty explicitly in hydrological and water  
101 quality modelling, not only through error bounds on output values, but by representing  
102 uncertainty as an intrinsic aspect of inexact environmental science (Beven, 2019; Pappenberger  
103 and Beven, 2006). Additionally, given the high levels of uncertainty and complexities involved  
104 in water quality mitigation and modelling, there is a pressing need to develop and apply  
105 probabilistic modelling tools for Environmental Risk Assessment (ERA) as an alternative to  
106 deterministic methods, and Bayesian Belief Networks (BBNs) are particularly well suited for  
107 this purpose (Moe et al., 2021). BBNs are a probabilistic graphical modelling framework that  
108 represents a set of variables and their conditional dependencies using a Directed Acyclic Graph  
109 (DAG) i.e., a network that has no cycles. BBNs are a powerful tool for modelling complex  
110 systems and have been used to integrate the disparate physicochemical, biotic/ abiotic, and  
111 socio-economic aspects (Penk et al., 2022) needed to simulate P in river catchments (Jarvie et  
112 al., 2019). BBNs show promise as decision support tools in water resource management (Phan  
113 et al., 2019) because they represent causal relationships between variables transparently and  
114 graphically, making it straightforward to understand and build BBNs with the participation of  
115 experts. BBNs facilitate an improved understanding of risk by explicitly representing the  
116 uncertainties and assumptions in the model as probability distributions, and they provide a  
117 systems-level understanding of a problem (Aguilera et al., 2011; Barton et al., 2012; Forio et  
118 al., 2015; Glendell et al., 2022; Kaikkonen et al., 2021; Kragt, 2009; Uusitalo, 2007). BBNs'  
119 can make predictions with sparse data (Forio et al., 2015; Glendell et al., 2022; Uusitalo, 2007);  
120 and the probabilistic outputs from BBNs can be used to recommend actions to policy makers,  
121 and to communicate best practices to stakeholders (Barton et al., 2012; Kaikkonen et al., 2021;  
122 Uusitalo, 2007). The probability distributions used in BBNs represent (most) model parameters  
123 explicitly encoding the uncertainties in the prior knowledge, data, and parameters (Sahlin et  
124 al., 2021). These prior distributions can be assumed, elicited from expert knowledge, or

125 measured using prior data. However, hybrid Bayesian Networks (BBNs that have a  
126 combination of continuous and discrete variables) are rarely applied in water quality modelling,  
127 and they have not been tested in a catchment with high-resolution monitoring data. Glendell et  
128 al., (2022) found that a hybrid BBN developed using standard regulatory data in seven test  
129 catchments in Scotland performed well, albeit with relatively large predictive uncertainty. In  
130 this work, we test whether a hybrid BBN can perform better when applied and calibrated in a  
131 catchment with long-term high-resolution data to understand whether the wide predictive  
132 uncertainty can be reduced or whether it is an irreducible property of this stochastic modelling  
133 approach. Hence, in this study we developed a BBN model of in-stream P concentrations in a  
134 poorly drained Irish agricultural catchment to: (1) model P losses in a data-rich meso-scale  
135 agricultural catchment using high-resolution observational data and expert advice; (2) evaluate  
136 the impact of rural point sources (septic tanks and farmyards), which are seldom represented  
137 in catchment water quality models, on P losses, and (3) evaluate the strengths and weaknesses  
138 of using BBNs as a modelling framework for high-resolution observational hydrological data.

139

## 140 **2. Materials and Methods**

### 141 2.1 Study area

142 This study focusses on the Ballycanew catchment (in older papers, also referred to as Grassland  
143 B, for example in Sherriff et al., (2015), Figure 1) located near Gorey, county Wexford, Ireland.  
144 The catchment covers 1207 ha and is comprised of 78% grassland and 20% tillage land use,  
145 while the remainder 2% is considered seminatural land use (Table 1). The catchment has been  
146 monitored intensively as part of the Agricultural Catchments Programme (ACP), Teagasc  
147 (Wall et al., 2011), which started in 2009 and is ongoing. Ballycanew soils have poor drainage  
148 characteristics due to deposits of heavy clays. However, landowners in the area have improved  
149 the land for grass production with tile and mole drainage. The low soil permeability in the

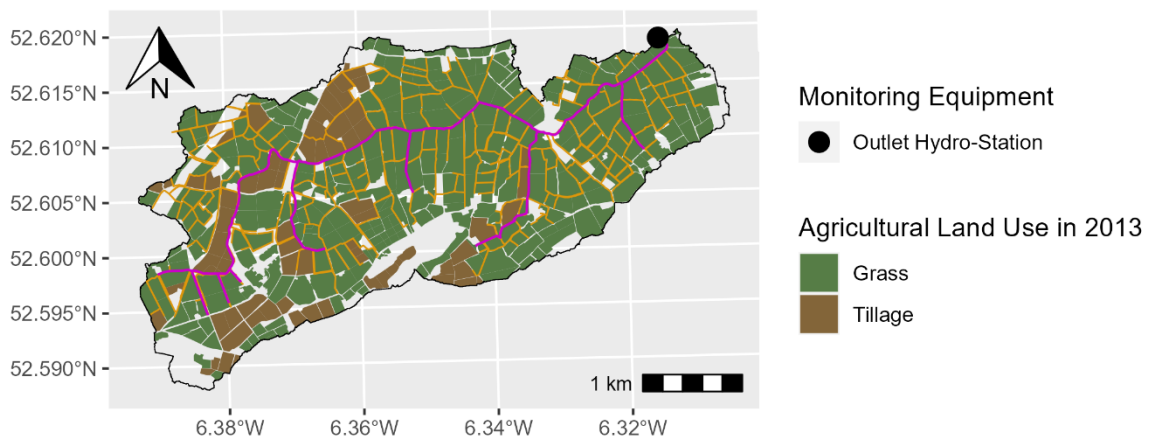
150 catchment results in flashy hydrology and a high risk of P loss to water through quick and  
151 erosive surface pathways during heavy rain events (Mellander et al., 2015).

152

## 153 2.2 Data collection

### 154 2.2.1 Hydrochemistry

155 The Ballycanew catchment is equipped with a river bank-side kiosk where the instrumentation  
156 is installed, its location is marked in Figure 1 as Outlet Hydro-Station (Mellander et al., 2012;  
157 Jordan et al., 2007). River water level is recorded every 10 minutes in a stilling well in the  
158 catchment outlet using an OTT Orpheus Mini vented-pressure instrument. The river discharge  
159 is calculated from a rating curve developed in a flat-V weir using an Acoustic Doppler Current  
160 meter. Total phosphorus (TP) and total reactive phosphorus (TRP) concentrations are  
161 monitored with a Hach-Lange Phosphax within the range of 0.01– 5.00 mg l<sup>-1</sup>, co-located with  
162 a Solitax Hach-Lange turbidity (turbidity units, NTU, also recorded every 10 minutes) sensor  
163 field-calibrated to suspended sediment concentration (mg l<sup>-1</sup>) (Sherriff et al., 2016).



164

165 *Figure 1 Study area: the Ballycanew catchment in County Wexford. Elevation varies between 21 m a.s.l. and 232 m a.s.l.*  
166 *The location of the hydrometric station is marked with the black dot, while magenta lines represent streams and yellow lines*  
167 *represent artificial drainage.*

168

169 Data from the bank-side monitoring station (Figure 1, Outlet Hydro-Station) collected every  
170 10 minutes (total discharge, average total reactive P concentrations, and average turbidity),  
171 were aggregated to daily average values for this study.

172

### 173 2.3 Bayesian Belief Network development

174 Bayesian Networks are directed acyclic graphs (DAGs), that represent a set of variables and  
175 their conditional dependencies using a graphical model. The term “directed acyclic” means that  
176 there is a sequential flow of information among variables and no dynamic feedback loops  
177 (Barton et al., 2012; Kragt, 2009). An introduction to Bayesian Networks and their application  
178 in ERA can be found in Moe et al., (2021), and won’t be repeated here. The relationships  
179 between variables in a BBN are parameterised using conditional probability distributions or  
180 conditional probability tables when variables are discrete (CPTs), and the graphical network is  
181 a description of such relationships (Borsuk et al., 2004). A hybrid Bayesian network combines  
182 both discrete and continuous variables, the latter represented as probability distributions. In  
183 this study, a conceptual BBN was developed in GeNIe 2.4 (BayesFusion, 2019) visualizing the  
184 ‘source-mobilisation-transport-continuum’ (Haygarth et al., 2005) and identifying the main  
185 drivers of phosphorus pollution in the catchment. The initial DAG comprised of 63 nodes and  
186 81 arcs, with 325 independent parameters out of 483, with parameter count defined as the total  
187 size of CPTs while independent parameters are those not implied by other parameters. The  
188 average number of node parents (indegree) was 1.3, and the maximum number of node parents  
189 was 5. An extensive literature review was conducted summarizing the knowledge base for the  
190 subject which was used to inform the priors (distribution shapes, and values) for key parameters  
191 in the models, as shown in Table 1. Catchment-specific information was also collated and used  
192 to inform the model structure and priors (Appendix A).



193 From the initial parameterization, two models were developed: Model A, which only accounts  
194 for diffuse reactive P sources (i.e., losses from soil matrix and topsoil), and Model B, which  
195 also includes P losses from farmyards, which is infrequent in P modelling (Harrison et al.,  
196 2019) and septic tanks, which are often overlooked as P sources, as opposed to centralized  
197 wastewater treatment centres (Withers et al., 2014). The models aim at integrating all the total  
198 reactive P losses from the different compartments at the catchment outlet (“Total catchment in-  
199 stream P load”,  $T \text{ month}^{-1}$ ) and then converting the loads into concentrations ( $\text{mg l}^{-1}$ ) by  
200 dividing by the monthly discharge ( $\text{m}^3 \text{ month}^{-1}$ ).

201

### 202 2.3.1 Expert input to inform key aspects of the model

203 Stakeholders and experts from the Agricultural Catchments Programme, the James Hutton  
204 Institute, and the Irish EPA with relevant areas of expertise (hydrology, hydrochemistry, land  
205 management, farm consultancy, policy making, and environmental modelling) were consulted  
206 in 1-to-1 meetings, and in a group workshop. Before the interviews and workshops, experts  
207 were provided with a topic information sheet describing the model and the aims and objectives  
208 of the session. The experts were asked to provide their input on the conceptual model structure  
209 to ensure that the causal dependencies between variables make sense and none were missing;  
210 characterizing the causal relationships; parameterising variables and their relationships using  
211 equations; approving the CPT values for the “Buffers” node, as well as deciding which loads  
212 were impacted by the buffer reduction (i.e., only surface-pathway derived nodes); and were  
213 asked to provide recommendations for further information sources (e.g., reports, publications,  
214 or datasets).

215

216 2.4 Model structure

217 The model structure is presented in Figure 2. The complete structure and specification of both  
218 models are included in Table 1 to allow reproducibility and further model application in  
219 different contexts. Table 1 describes the model structure and informs on the conditional  
220 probability distributions as well as which CPTs were logical, expert-approved, and which were  
221 derived from data or literature, also highlighting which sub-models and variables are part of  
222 Model A or Model B. In particular, the “Hydrology”, “Management”, and “Erosion” sub-models  
223 are represented in both Model A and B, while the sub-models for septic tanks and farmyards  
224 are only represented in Model B.

225 Table 1 Model specifications organized by sub-model. The “Hydrology”, “Management”, and “Erosion” sub-models belong to both Model A and B.

Variable (symbol) [unit]	States	Discretisation boundaries/ Probability	Description
<b>Hydrology sub-model (Drivers)</b>			
Month	Each month		Calculated as No. days in the month/ 365
Calculated variables			
Mean total monthly Q (discharge) [m <sup>3</sup> ]	Very Low	0-109424	Bootstrapped from daily total discharge observations (2009-2016) to obtain a Lognormal ( $\mu$ ; $\sigma$ ) discharge distribution with base e for each month. Each month’s parameters are shown in the table. Discretization of states is based on percentiles calculated from the average monthly observations (very low $\leq$ 5 <sup>th</sup> percentile, low= 5 <sup>th</sup> -25 <sup>th</sup> percentile, medium= 25 <sup>th</sup> -50 <sup>th</sup> percentile, high= 50 <sup>th</sup> -75 <sup>th</sup> percentile, very high= 75 <sup>th</sup> -100 <sup>th</sup> percentile).
	Low	109424-227082	
	Medium	227082-373942	
	High	373942-806788	
	Very High	806788-1124380	
Mean total monthly Surface Flow (surface runoff) [m <sup>3</sup> ]	Very Low	0-28450	Calculated as a portion of mean monthly runoff (26%), via hydrograph separation method described in Mellander et al., (2012). Discretization of states is based on percentiles calculated from observations (very low $\leq$ 5 <sup>th</sup> percentile, low= 5 <sup>th</sup> -25 <sup>th</sup> percentile, medium= 25 <sup>th</sup> -50 <sup>th</sup> percentile, high= 50 <sup>th</sup> -75 <sup>th</sup> percentile, very high= 75 <sup>th</sup> -100 <sup>th</sup> percentile).
	Low	28450-59042	
	Medium	59042-97225	
	High	97225-209765	
	Very High	209765-292338	
	Very Low	0-19696	

	$\mu$	$\sigma$
<b>January</b>	13.8	0.17
<b>February</b>	13.5	0.18
<b>March</b>	12.9	0.17
<b>April</b>	12.5	0.19
<b>May</b>	12.2	0.21
<b>June</b>	11.8	0.30
<b>July</b>	11.3	0.32
<b>August</b>	11.8	0.50
<b>September</b>	11.5	0.36
<b>October</b>	12.8	0.40
<b>November</b>	13.7	0.21
<b>December</b>	13.8	0.21

Mean total monthly Sub-surface Stormflow (subsurface runoff) [m <sup>3</sup> ]	Low	19696-40875	Calculated as a portion of mean monthly runoff (18%), via hydrograph separation method described in Mellander et al., (2012). Discretization of states is based on percentiles calculated from observations (very low<= 5 <sup>th</sup> percentile, low= 5 <sup>th</sup> -25 <sup>th</sup> percentile, medium= 25 <sup>th</sup> -50 <sup>th</sup> percentile, high= 50 <sup>th</sup> -75 <sup>th</sup> percentile, very high= 75 <sup>th</sup> -100 <sup>th</sup> percentile).																
	Medium	40875-67309																	
	High	67309-145222																	
	Very High	145222-202388																	
Mean total monthly Baseflow [m <sup>3</sup> ]	Very Low	0-61277	Calculated as a portion of mean monthly runoff (56%), via hydrograph separation method described in Mellander et al., (2012). Discretization of states is based on percentiles calculated from observations (very low<= 5 <sup>th</sup> percentile, low= 5 <sup>th</sup> -25 <sup>th</sup> percentile, medium= 25 <sup>th</sup> -50 <sup>th</sup> percentile, high= 50 <sup>th</sup> -75 <sup>th</sup> percentile, very high= 75 <sup>th</sup> -100 <sup>th</sup> percentile).																
	Low	61277-127166																	
	Medium	127166-209407																	
	High	209407-451801																	
	Very High	451801-629651																	
<b>Management (Drivers)</b>																			
Land use	Arable	0.20	As reported by Teagasc - Agriculture and Food Development Authority, (2018).																
	Grassland	0.78																	
	Seminatural	0.02																	
Buffers	<table border="1"> <thead> <tr> <th>Land use</th> <th>Arable</th> <th>Grassland</th> <th>Seminatural</th> </tr> </thead> <tbody> <tr> <td>2 m</td> <td>0.98</td> <td>1.01E-06</td> <td>1.01E-06</td> </tr> <tr> <td>&gt;2 m</td> <td>0.019</td> <td>1.01E-06</td> <td>1.01E-06</td> </tr> <tr> <td>none</td> <td>0.001</td> <td>0.999</td> <td>0.999</td> </tr> </tbody> </table>		Land use	Arable	Grassland	Seminatural	2 m	0.98	1.01E-06	1.01E-06	>2 m	0.019	1.01E-06	1.01E-06	none	0.001	0.999	0.999	Buffers are defined as being 2 m in width, more than 2 m in width, or absent. Probabilities of having either type of buffer according to land use were agreed upon with one of the ACP advisors during consultation.
Land use	Arable	Grassland	Seminatural																
2 m	0.98	1.01E-06	1.01E-06																
>2 m	0.019	1.01E-06	1.01E-06																
none	0.001	0.999	0.999																
<b>Calculated variables</b>																			
Buffer effectiveness for Particulate P (PP) and suspended sediments (SS)	Very Low	0-0.2	Dependent on the variable Buffers. For 2 m buffers, effectiveness is defined as Beta ( $\alpha=2.9$ ; $\beta=4.5$ ); for >2 m buffers it is defined as Beta ( $\alpha=1.44$ ; $\beta=0.789$ ); for no buffers, effectiveness is equal to 0. The distributions were fitted to the dataset published in Stutter et al., (2021), where negative retention data was deleted from the analysis.																
	Low	0.2-0.4																	
	Medium	0.4-0.6																	
	High	0.6-0.8																	
	Very High	0.8-1																	
Buffer effectiveness for Total Dissolved P (TDP)	Very Low	0-0.2	Dependent on the variable Buffers. For Buffers 0-2 m, Buffer effectiveness is defined as Beta ( $\alpha=1.8$ ; $\beta=2.7$ ), for >2 m buffers it is defined as Beta ( $\alpha=1$ ; $\beta=0.8$ ); for no buffers, effectiveness is equal to 0. The distributions were fitted to the dataset published in Stutter et al., (2021), where negative retention data was deleted from the analysis.																
	Low	0.2-0.4																	
	Medium	0.4-0.6																	
	High	0.6-0.8																	
	Very High	0.8-1.0																	
<b>Soil erosion and soil P sub-model</b>																			
Morgan P	<table border="1"> <thead> <tr> <th></th> <th>Arable</th> <th>Grassland</th> <th>Seminatural</th> </tr> </thead> <tbody> <tr> <td><b>Morgan1</b></td> <td>0.47</td> <td>0.46</td> <td>0</td> </tr> </tbody> </table>			Arable	Grassland	Seminatural	<b>Morgan1</b>	0.47	0.46	0	Based on land use, proportions of land for each level and in each land use category were calculated based on the soil survey carried out in 2013 in the								
	Arable	Grassland	Seminatural																
<b>Morgan1</b>	0.47	0.46	0																

		<b>Morgan2</b>	0.42	0.35	0.6	catchment. Where the Morgan P index was unknown, that proportion of land was assigned to the dominant index category. For the interpretation of the Soil Morgan P Index, the reader is referred to Regan et al., (2012).																																							
		<b>Morgan3</b>	0.09	0.14	0.3																																								
		<b>Morgan4</b>	0.02	0.05	0.1																																								
<b>Calculated variables</b>																																													
Monthly Turbidity [NTU month <sup>-1</sup> ]	Very Low	0-1402		<p>Bootstrapped from daily average turbidity observations (2009-2016) to obtain a Lognormal (<math>\mu</math>; <math>\sigma</math>) turbidity distribution with base e for each month. Each month's parameters are shown in the table. Discretization of states is based on percentiles calculated from the average monthly observations (very low <math>\leq</math> 5<sup>th</sup> percentile, low = 5<sup>th</sup>-25<sup>th</sup> percentile, medium = 25<sup>th</sup>-50<sup>th</sup> percentile, high = 50<sup>th</sup>-75<sup>th</sup> percentile, very high = 75<sup>th</sup>-100<sup>th</sup> percentile).</p> <table border="1"> <thead> <tr> <th></th> <th><math>\mu</math></th> <th><math>\sigma</math></th> </tr> </thead> <tbody> <tr><td><b>January</b></td><td>6.3</td><td>0.25</td></tr> <tr><td><b>February</b></td><td>6.0</td><td>0.23</td></tr> <tr><td><b>March</b></td><td>5.6</td><td>0.23</td></tr> <tr><td><b>April</b></td><td>5.5</td><td>0.20</td></tr> <tr><td><b>May</b></td><td>5.3</td><td>0.15</td></tr> <tr><td><b>June</b></td><td>5.5</td><td>0.15</td></tr> <tr><td><b>July</b></td><td>5.2</td><td>0.13</td></tr> <tr><td><b>August</b></td><td>5.2</td><td>0.13</td></tr> <tr><td><b>September</b></td><td>5.2</td><td>0.12</td></tr> <tr><td><b>October</b></td><td>5.7</td><td>0.24</td></tr> <tr><td><b>November</b></td><td>6.2</td><td>0.30</td></tr> <tr><td><b>December</b></td><td>6.2</td><td>0.30</td></tr> </tbody> </table>				$\mu$	$\sigma$	<b>January</b>	6.3	0.25	<b>February</b>	6.0	0.23	<b>March</b>	5.6	0.23	<b>April</b>	5.5	0.20	<b>May</b>	5.3	0.15	<b>June</b>	5.5	0.15	<b>July</b>	5.2	0.13	<b>August</b>	5.2	0.13	<b>September</b>	5.2	0.12	<b>October</b>	5.7	0.24	<b>November</b>	6.2	0.30	<b>December</b>	6.2	0.30
		$\mu$	$\sigma$																																										
	<b>January</b>	6.3	0.25																																										
	<b>February</b>	6.0	0.23																																										
	<b>March</b>	5.6	0.23																																										
<b>April</b>	5.5	0.20																																											
<b>May</b>	5.3	0.15																																											
<b>June</b>	5.5	0.15																																											
<b>July</b>	5.2	0.13																																											
<b>August</b>	5.2	0.13																																											
<b>September</b>	5.2	0.12																																											
<b>October</b>	5.7	0.24																																											
<b>November</b>	6.2	0.30																																											
<b>December</b>	6.2	0.30																																											
Low	1402-1665																																												
Medium	1665-2270																																												
High	2270-3391																																												
Very High	3391-4344																																												
Monthly Suspended Sediment concentration [mg l <sup>-1</sup> month <sup>-1</sup> ]	Very Low	0-133.3		<p>Calculated as: <math>a * \text{Monthly Turbidity [NTU month}^{-1}]^b</math>, where <math>a = 0.567</math>, and <math>b = 1.1109</math>, as described in Sherriff et al., (2015). Discretization of states is based on percentiles calculated from the average monthly calculated observations (very low <math>\leq</math> 5<sup>th</sup> percentile, low = 5<sup>th</sup>-25<sup>th</sup> percentile, medium = 25<sup>th</sup>-50<sup>th</sup> percentile, high = 50<sup>th</sup>-75<sup>th</sup> percentile, very high = 75<sup>th</sup>-100<sup>th</sup> percentile).</p>																																									
	Low	133.3-165																																											
	Medium	165-237.6																																											
	High	237.6-369.3																																											
	Very High	369.3-480.0																																											
Water Extractable P (WEP) [mg l <sup>-1</sup> ]	Low	0-3		Based on variable "Morgan P levels" and "land use" (data from 2013) it is calculated with the																																									
	Medium	3-5																																											

	High	5-8	<p>equations available in (Thomas et al., 2016b): for Grassland, <math>WEP=0.60 * Morgan P + 1.46</math>, for Arable: <math>WEP= 0.45 * Morgan P + 0.19</math>, where Morgan P is defined as a Uniform distribution with the following parameters:</p> <table border="1"> <thead> <tr> <th>Morgan P Index</th> <th>Grassland</th> <th>Arable</th> </tr> </thead> <tbody> <tr> <td>Index 1</td> <td>a=0; b=3</td> <td>a=0; b=3</td> </tr> <tr> <td>Index 2</td> <td>a=3.1; b=5</td> <td>a=3.1; b=6</td> </tr> <tr> <td>Index 3</td> <td>a=5.1; b=8</td> <td>a=6.1; b=10</td> </tr> <tr> <td>Index 4</td> <td>a=8.1; b=30</td> <td>a=10.1; b=30</td> </tr> </tbody> </table> <p>For the Seminalural Land use, WEP was assumed constant to 0.001. Discretization is based on Morgan P discrete levels.</p>	Morgan P Index	Grassland	Arable	Index 1	a=0; b=3	a=0; b=3	Index 2	a=3.1; b=5	a=3.1; b=6	Index 3	a=5.1; b=8	a=6.1; b=10	Index 4	a=8.1; b=30	a=10.1; b=30
	Morgan P Index	Grassland		Arable														
Index 1	a=0; b=3	a=0; b=3																
Index 2	a=3.1; b=5	a=3.1; b=6																
Index 3	a=5.1; b=8	a=6.1; b=10																
Index 4	a=8.1; b=30	a=10.1; b=30																
Very High	8-15																	
Sediment Water Soluble P [mg kg <sup>-1</sup> ]	Very Low	0-0.0995	<p>Defined as a Lognormal distribution (<math>\mu=-0.9</math>, <math>\sigma=1</math>), fitted with the <i>SHELF</i> R package (version 1.8.0, Oakley, 2020) to observed Water Extractable P in the catchment sediments (Shore et al., 2016). Discretization of states is based on percentiles calculated from the observations (very low <math>\leq</math> 5<sup>th</sup> percentile, low= 5<sup>th</sup>-25<sup>th</sup> percentile, medium= 25<sup>th</sup>-50<sup>th</sup> percentile, high= 50<sup>th</sup>-75<sup>th</sup> percentile, very high= 75<sup>th</sup>-100<sup>th</sup> percentile).</p>															
	Low	0.0995-0.2100																
	Medium	0.2100-0.3550																
	High	0.3550-0.9100																
	Very High	0.9100-8																
Predicted Dissolved P Concentration [mg l <sup>-1</sup> ]	Low	0-3	<p>Dependant on Water Extractable P, it is defined with the linear model: Predicted Dissolved P = <math>\beta(WEP)+\alpha</math>, where <math>\beta =0.08</math>, <math>\alpha =0.158</math>, derived from (Thomas et al., 2016b). This equation is derived from data gathered during the closed period only, that is, when farmers are forbidden from spreading fertilizer. An assumption is made that when the linear model yields a negative value, that is resampled as a zero. Water Extractable P is considered a good in-stream TRP/ TDP predictor in the ACP catchments by the experts, however careful consideration is needed when choosing a soil P test in a different setting.</p>															
	Medium	3-5																
	High	5-8																
	Very High	8-15																
Sub-surface Dissolved P load [kg month <sup>-1</sup> ]	Low	0-3	<p>Calculated as the product of Predicted Dissolved P concentration and Subsurface Storm-flow.</p>															
	High	3-200																
Baseflow Dissolved P load	Low	0-3																

[kg month <sup>-1</sup> ]	High	3-200	Calculated as the product of Predicted Dissolved P concentration and Baseflow.
Modified Dissolved P load [kg month <sup>-1</sup> ]	Low	0-3	Based on “Buffer effectiveness for Total Dissolved P”, for effective buffers, modified Dissolved P load= Sub-surface Dissolved P load *(1-Buffer effectiveness for TDP).
	High	3-200	
Monthly Sediment P load [kg month <sup>-1</sup> ]	Low	0-3	Calculated as the product of Sediment Water Soluble P [mg kg <sup>-1</sup> ], Monthly Suspended Sediment concentration [mg l <sup>-1</sup> month <sup>-1</sup> ], and Mean total monthly surface flow [m <sup>3</sup> ].
	High	3-200	
Modified Sediment P load [kg month <sup>-1</sup> ]	Low	0-3	Based on “Buffer effectiveness for Suspended Sediments and Particulate P”, for effective buffers, Modified Sediment P load= Monthly Sediment P load [kg month <sup>-1</sup> ]*(1-Buffer effectiveness for SS and PP).
	High	3-200	
<b>Septic Tanks (ST) sub-model (Point P sources), included in Model B only</b>			
P concentration per tank [mg l <sup>-1</sup> ]	Absent (to represent 0 STs)	0-1*10 <sup>-8</sup>	P concentration is dependent on the treatment type. If the treatment is unknown, the concentration is defined as a Lognormal distribution ( $\mu=2.9$ , $\sigma=1.25$ ), based on a literature review of data available for Ireland (Environmental Protection Agency Ireland (EPA), 2003, 2000; Gill et al., 2005, 2007) (n=8). Fitting was done with R package <i>fitdistrplus</i> (version 1.1-8, Delignette-Muller et al., 2020). Otherwise, for primary and secondary treatment concentration is defined as Truncated Normal distribution ( $\mu=10$ ; $\sigma=1$ ), and ( $\mu=5$ ; $\sigma=0.5$ ) respectively, as described in Glendell et al., (2021) and derived from SEPA guidelines (Brownlie et al., 2014). All tanks are assumed to be maintained. Discretization was also based on the literature review.
	Low	1*10 <sup>-8</sup> -1	
	Medium	1-18	
	High	18-35	
	Very High	35-100	
<b>Management related variables</b>			
Direct discharge	Present	0.16	Probabilities are derived from the report by the Environmental Protection Agency Ireland (EPA, 2015).
	Absent	0.84	
Treatment	Unknown	0.50	Probability of having “unknown”, “primary” or “secondary” treatment of the effluent in a septic tank. Probabilities based on a survey conducted within WaterProtect, a research project supported by the European Union research and innovation
	Primary	0.31	
	Secondary	0.19	

									funding programme Horizon 2020 [grant no. 727450].		
<b>Connectivity related variables</b>											
Degree of Phosphorus Saturation (DPS) [%]	Very Low_0_20								0.978	Discretization is equal to the 20 <sup>th</sup> , 40 <sup>th</sup> , 60 <sup>th</sup> , and 80 <sup>th</sup> quantiles, however 0 < DPS < 60 in this catchment. Probabilities were calculated from available spatial data (Wall et al., 2012).	
	Medium_20_40								0.017		
	High_40_60								0.005		
Soil risk factor [adimensional]	Very Low								9.9*10 <sup>-6</sup>	An indicator to describe the combined risk of effluent leaching to the groundwater table with the risk of the effluent being transported with surface runoff. This approach is a simplification of the one adopted in Glendell et al., (2021). The risk factor was obtained by overlaying the soil series (Thomas et al., 2016a) with information on the position of the groundwater table (0- 2 m below ground or more than 2 m below ground). As little is known regarding the septic tanks in the catchment (i.e. age, type of treatment, maintenance), a conservative approach was applied here to obtain higher risk classes. The table to the left represents a synthesis of the classification approach. Probabilities are based on land cover proportion.	
	Low								0.370		
	Medium								9.9*10 <sup>-6</sup>		
	High								0.620		
	Very High								0.006		
				<b>Groundwater Table Position</b>							
				<b>Soil Series</b>	<b>0-2 m below surface</b>	<b>&gt;2 m below surface</b>					
			<b>Brown earths</b>	High Risk	Moderate Risk						
			<b>Alluvial</b>	High Risk	Moderate Risk						
			<b>Luvisol</b>	High Risk	Moderate Risk						
			<b>Gley</b>	Very High Risk	Very High Risk						
Leachfield removal			<b>Soil risk factor</b>	<b>DPS</b>	<b>Low</b>	<b>Medium</b>	<b>High</b>				
			<b>Very low</b>	<b>Very Low</b>	0.0	0.0	1.0				
				<b>Medium</b>	0.0	0.5	0.5				
				<b>High</b>	0.5	0.5	0.0				
			<b>Low</b>	<b>Very Low</b>	0.0	0.3	0.7				
				<b>Medium</b>	0.0	0.7	0.3				
				<b>High</b>	0.3	0.7	0.0				
			<b>Medium</b>	<b>Very Low</b>	0.0	0.5	0.5				
				<b>Medium</b>	0.0	1.0	0.0				
				<b>High</b>	0.5	0.5	0.0				
			<b>High</b>	<b>Very Low</b>	0.0	0.7	0.3				
				<b>Medium</b>	0.3	0.7	0.0				
				<b>High</b>	0.7	0.3	0.0				
			<b>Very High</b>	<b>Very Low</b>	0.0	0.5	0.5				
				<b>Medium</b>	0.5	0.5	0.0				
<b>High</b>	1.0	0.0		0.0							
The node refers to P removal from septic drains. Conditional on P leaching risk from Degree of Phosphorus Saturation (DPS). The conditional probability table is a logical one.											



Leachfield connectedness		<b>HSA rescaled</b>	<b>None</b>		<b>Low</b>		<b>Medium</b>		<b>High</b>		Probabilities are conditional on the presence/absence of Direct ST discharge, and HSA (node: Connectivity rescaled HSA). Where Direct discharge is present, connectedness is assumed as 'high'. Where Direct discharge is absent, the risk class of the HSA is assigned.
		<b>Direct discharge</b>	<b>pres</b>	<b>abs</b>	<b>pres</b>	<b>abs</b>	<b>pres</b>	<b>abs</b>	<b>pres</b>	<b>abs</b>	
		<b>low</b>	0	1	0	1	0	0	0	0	
		<b>medium</b>	0	0	0	0	0	1	0	0	
		<b>high</b>	1	0	1	0	1	0	1	1	
Septic Tank connectedness	<b>Leachfield removal</b>	<b>Low</b>			<b>Medium</b>			<b>High</b>			Probabilities are conditional on Leachfield removal and Leachfield connectedness. Where Leachfield removal is 'low' or 'High', Leachfield connectedness remains unaltered.
	<b>Leachfield connectedness</b>	<b>Low</b>	<b>Medium</b>	<b>High</b>	<b>Low</b>	<b>Medium</b>	<b>High</b>	<b>Low</b>	<b>Medium</b>	<b>High</b>	
	<b>Low</b>	1.0	0.0	0.0	1.0	0.0	0.0	1.0	0.5	0.0	
	<b>Medium</b>	0.0	1.0	0.0	0.0	1.0	0.5	0.0	0.5	1.0	
	<b>High</b>	0.0	0.0	1.0	0.0	0.0	0.5	0.0	0.0	0.0	
Connectivity rescaled [adimensional]	HSA	None_0					0.60				Data extracted from spatial layers of Hydrologically Sensitive Areas (HSAs) provided by the Agricultural Catchments Programme (Thomas et al., 2016b). Discretization is also based on the spatial layers.
		Low_1_3					0.18				
		Medium_4_7					0.20				
		High_8_10					0.02				
<b>Calculated variables</b>											
Load per tank [kg month <sup>-1</sup> ]	Absent					0-1*10 <sup>-6</sup>					Specified as the product of ST density [No ha <sup>-1</sup> ] * ST concentration [mg l <sup>-1</sup> ] * 120 [L] average daily water consumption per person * 365/12 days in a month* average No of persons per household 2.7/1*10 <sup>6</sup> . Discretisation is based on interpolation to represent plausible probabilities for combination of extreme risk classes (eg. High+high=high, low+low=low).
	Very Low					1*10 <sup>-6</sup> -0.1					
	Low					0.1-0.5					
	Medium					0.5-1.0					
	High					1.0-2.0					
	Very High					2.0-30					
Total Realized load [T month <sup>-1</sup> ]	Very Low					0.0-0.1					Calculated as the product of septic tank load and delivery factors (D) related to the connectedness of a septic tank, based on the median estimated fraction to be delivered in Table 13 of the report by Glendell et al., (2021) and the number of septic tanks present within catchment boundary (N): Realised load per tank [kg month <sup>-1</sup> ] * N * D / 1000. In this case, N= 88. Discretisation based on interpolation to represent plausible probabilities for combination of extreme risk classes.
	Low					0.1-0.5					
	Medium					0.5-1.0					
	High					1.0-2.0					
	Very High					2.0-12					
		<b>Septic tank connectedness</b>	<b>Delivery factor (D)</b>			<b>Reference</b>					
	<b>Low</b>	0.05			"very low" category in Appendix A3, Glendell et al., (2021)						
	<b>Medium</b>	0.30			"medium" category in Appendix A3, Glendell et al., (2021)						

		<b>High</b>	0.80	“very high” category in Appendix A3, Glendell et al., (2021)	
<b>Farmyards sub-model (Point P sources), included in Model B only</b>					
Farmyard size area [m <sup>2</sup> ]	Very Low		0-56	Based on available farmyard survey, a distribution was fitted to farmyard area data: Lognormal ( $\mu=-5.6$ ; $\sigma=0.98$ ). Discretization of states is based on percentiles calculated from the observations (very low $\leq$ 5 <sup>th</sup> percentile, low= 5 <sup>th</sup> -25 <sup>th</sup> percentile, medium= 25 <sup>th</sup> -50 <sup>th</sup> percentile, high= 50 <sup>th</sup> -75 <sup>th</sup> percentile, very high= 75 <sup>th</sup> -100 <sup>th</sup> percentile).	
	Low		56-127		
	Medium		127-277		
	High		277-586		
	Very High		586-4500		
Farmyard P concentration [mg l <sup>-1</sup> ]	Very Low		0-0.01	Using the <i>SHELF</i> R package (version 1.8.0, Oakley, 2020), a distribution was fitted to the data in Table 2 in Harrison et al., (2019): Lognormal ( $\mu=-1.8$ ; $\sigma=1.6$ ). The best fit would have been the LogT distribution, however, that is not available for Genie, so we opted for Lognormal. Discretization is also based on the literature. For simplicity, here we have used SRP to mean TRP.	
	Low		0.01-0.50		
	Medium		0.50-1.00		
	High		1.00-2.50		
	Very High		2.50-30		
Incidental losses per average yard [kg month <sup>-1</sup> ]	Very Low		$0-1 \times 10^{-9}$	Based on average farmyard size, losses are calculated as Surface runoff [m <sup>3</sup> ] / catchment area [m <sup>2</sup> ] * Farmyard size area [m <sup>2</sup> ] * Farmyard P concentration [mg l <sup>-1</sup> ] / 10 <sup>3</sup> .	
	Low		$1 \times 10^{-9}$ -0.001		
	Medium		0.001-0.01		
	High		0.01-0.10		
	Very High		0.10-60		
Total incidental losses [T month <sup>-1</sup> ]	Very Low		$0-1 \times 10^{-5}$	Incidental losses per average yard [kg month <sup>-1</sup> ] * N, where N is the total number of yards present within the catchment boundary. In this case, N =70.	
	Low		1e-05-0.007		
	Medium		0.007-0.070		
	High		0.07-0.700		
	Very High		0.700-420		
<b>Catchment outlet integration sub-model</b>					
Total catchment in-stream P load [T month <sup>-1</sup> ]	Low		0-0.02	Equal to the sum of Baseflow Dissolved P load [kg month <sup>-1</sup> ], Modified Dissolved P load [kg month <sup>-1</sup> ], Modified Sediment P load [kg month <sup>-1</sup> ], Total incidental losses [T month <sup>-1</sup> ], and Total Realized load [T month <sup>-1</sup> ], all converted to appropriate units.	
	Medium		0.02-1		
	High		1-10		
In-stream P concentration [mg l <sup>-1</sup> ]	Good		0-0.035	Defined as the Total catchment in-stream P load [T] * 10 <sup>9</sup> / Mean total monthly Q (discharge) [m <sup>3</sup> ] * 1000, where mean monthly discharge is equal to the total catchment discharge measured at the outlet.	
	Bad		0.035-10		

Environmental Quality Standard [TRP concentration mg l <sup>-1</sup> ]	<table border="1"> <thead> <tr> <th data-bbox="871 213 1064 268">TRP concentration</th> <th data-bbox="1064 213 1182 268">Good</th> <th data-bbox="1182 213 1310 268">Bad</th> </tr> </thead> <tbody> <tr> <td data-bbox="871 268 1064 306">Good</td> <td data-bbox="1064 268 1182 306">1</td> <td data-bbox="1182 268 1310 306">0</td> </tr> <tr> <td data-bbox="871 306 1064 344">Bad</td> <td data-bbox="1064 306 1182 344">0</td> <td data-bbox="1182 306 1310 344">1</td> </tr> </tbody> </table>	TRP concentration	Good	Bad	Good	1	0	Bad	0	1	Discretization of the variable “In-stream TRP concentration [mg l <sup>-1</sup> ]”. For simplicity, in-stream TRP is here considered equal to in-stream Dissolved Reactive Phosphorus, as in previous studies the mean DRP accounted for 98–99% of the flow-weighted mean TRP (Shore et al., 2014).
TRP concentration	Good	Bad									
Good	1	0									
Bad	0	1									

## 227 2.5 Model evaluation

228 P models typically struggle to produce positive performance indicators (Jackson-Blake et al.,  
229 2015). Therefore, the model performance was evaluated following the procedures suggested  
230 by Jackson-Blake et al., (2015), using a suite of strategies comparing predicted TRP  
231 concentrations ( $\text{mg l}^{-1}$ ) with the observed TRP concentrations (available as daily average,  $\text{mg}$   
232  $\text{l}^{-1}$ ) (1/10/2009-31/12/2016) by 1) calculating percentage bias (PBIAS), 2) comparing summary  
233 statistics (median, mean, upper and lower limit, interquartile ranges), and 3) comparing the full  
234 posterior distributions with the observations. Using the R *SHELF* package (version 1.8.0,  
235 Oakley, 2020), a monthly lognormal distribution was fitted to the observed TRP concentrations  
236 using 100 quantiles and 0 as the lower limit. This distribution was used to compute the PBIAS  
237 % in the R package *hydroGOF* (version 0.4-0, Zambrano-Bigiarini, 2020). In addition, a  
238 bootstrapping method was applied to the available observations to obtain a lognormal  
239 distribution fitted to each month's TRP concentration data. Percentage bias was used to  
240 evaluate the BBNs performances in each month, in this case with 10,000 data points simulated  
241 in the BBNs by selecting each month as evidence, and 10,000 data points drawn from each  
242 month's lognormal distribution fitted to the observational data using bootstrapping. Both for  
243 the overall and the monthly performance evaluation, data points outside the instrument's limits  
244 of detection ( $0.01 - 5.00 \text{ mg l}^{-1}$ ) were excluded from the model evaluation.

245

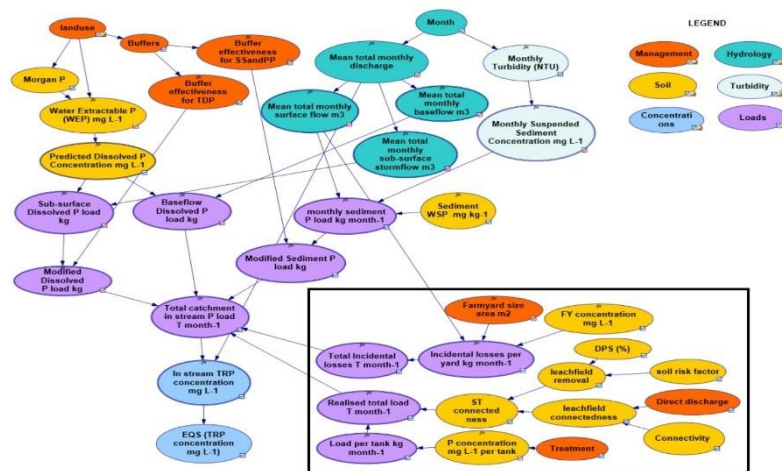
## 246 **3. Results and discussion**

### 247 3.1 Model structure

248 As a result of the discussions with experts, the final model is considerably less complex than  
249 was initially conceptualized. As mentioned, the original BBN comprised 63 nodes and 81 arcs,  
250 while the resulting Model B comprises 38 nodes, 46 arcs, 106 independent parameters out of  
251 153, average indegree of 1.2, and maximum indegree of 5. The final BBN structure is shown

252 in Figure 2, which highlights which nodes were part of Model A and which ones were added  
 253 for Model B. The model structure (Table 1) directly reports which variables were influenced  
 254 by experts, in an attempt to address some of the transparency issues raised by Kaikkonen et al.,  
 255 (2021) regarding expert role.

256



257

258 *Figure 2 Structure of the final BBNs, including the additional nodes for Model B highlighted inside the box.*

259

### 260 3.2.1 Phosphorus concentrations in the stream – overall performance

261 Overall model performance is shown in Table 2, where mean, lower and upper limit, and  
 262 meaningful percentiles of the BBN TRP concentration distributions are shown against the  
 263 average monthly distribution fitted to the observations. The 5<sup>th</sup> percentile shows that the model  
 264 concentrations are more skewed towards low concentrations than the observations. This may  
 265 be related to the equation used to calculate the variable “Predicted Dissolved P Concentration  
 266 [mg l<sup>-1</sup>]”, reported in Table 1 and derived from Thomas et al., (2016b). The node was set up to  
 267 substitute the negative values with zeroes (because the equation would allow negative P  
 268 concentrations). In fact, 25% of the simulated values for the “Predicted Dissolved P

269 Concentration [ $\text{mg l}^{-1}$ ]” node equalled zero (meaning no TRP from the soil matrix would be  
 270 measured at the catchment outlet) and currently included when computing the final TRP  
 271 concentration distribution prior to censoring it by instrument’s limits of detection (0.01– 5.00  
 272  $\text{mg l}^{-1}$ ), which may have skewed the model predictions. However, the model results are also  
 273 skewed towards larger concentrations in the upper percentiles compared to the observations.  
 274 The median modelled TRP concentration approximates the observed median, and as discussed,  
 275 the tails of the modelled distributions are wider than those in observed mean daily data, which  
 276 is also shown in Figure 3.

277

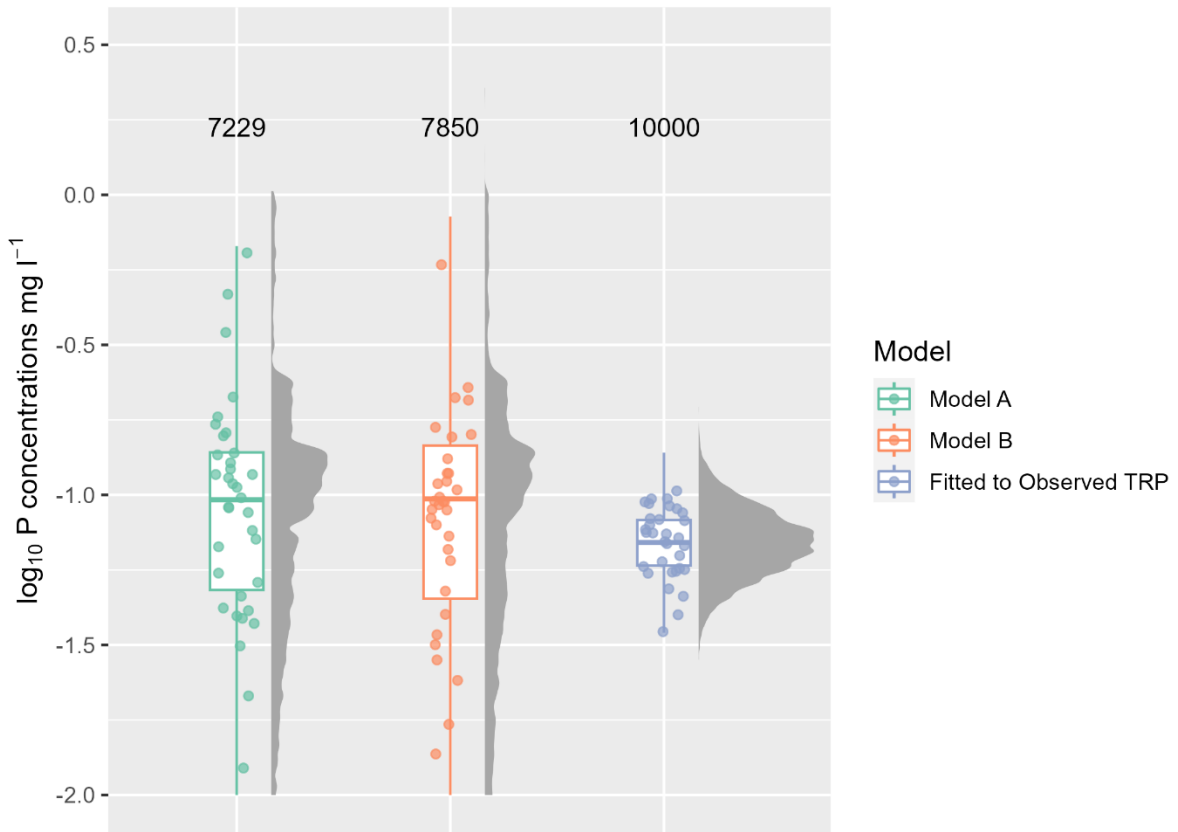
278 *Table 2 The two model’s overall performances in terms of mean, standard deviation, quantiles, and percentage bias. Data*  
 279 *outside the instrument’s limit of detection (0.01-5.00  $\text{mg l}^{-1}$ ) were excluded from the calculations. Both observed and*  
 280 *predicted TRP concentrations were log-transformed before calculating the statistics, and then converted back to normal*  
 281 *values.*

	<b>Observed TRP (time-weighted)</b>	<b>Predicted TRP Diffuse P (flow-weighted)</b>	<b>Predicted TRP Diffuse + Point P (flow-weighted)</b>
		<b><math>\text{mg l}^{-1}</math></b>	
<b>lower limit (<math>\mu-1\sigma</math>)</b>	0.03	0.03	0.03
<b>mean</b>	0.06	0.08	0.08
<b>upper limit (<math>\mu+1\sigma</math>)</b>	0.10	0.20	0.21
<b>5<sup>th</sup> percentile</b>	0.02	0.02	0.01
<b>25<sup>th</sup> percentile</b>	0.04	0.05	0.04
<b>50<sup>th</sup> percentile</b>	0.06	0.09	0.10
<b>75<sup>th</sup> percentile</b>	0.08	0.14	0.14
		<b>Model A (Diffuse P)</b>	<b>Model B (Diffuse + Point P)</b>
<b>Percentage bias against distribution fitted to observations (%)</b>	-	76	80

282

283

284 Figure 3 shows the overall model distributions compared to the lognormal distribution fitted to  
 285 the observations. The boxplots and the density plots at their right-hand side show the full  
 286 distributions excluding data points outside the instrument’s limit of detection, while the dots  
 287 scattered on top of the boxplots show only a sample ( $n = 30$ ).



288

289 *Figure 3 Overall distribution density of  $\log_{10}$  TRP concentrations fitted to observations versus those predicted by the two*  
 290 *developed BBNs. BBN predictions show a larger variance, the full extent of which is shown in the plot by the density and box*  
 291 *plots and scattered data points. Data outside the instrument's limit of detection ( $0.01\text{-}5.00 \text{ mg l}^{-1}$ ) were excluded from the*  
 292 *plot, and the text shows the number of valid samples for each model. This plot was produced with the ggdist R package*  
 293 *version 3.3.0 (Kay, 2023).*

294

295

296 3.2.2 Phosphorus concentrations in the stream – monthly performance

297 Each month's modelled and observed TRP concentrations are shown as histogram plots in  
298 Figure 4 A and as density plots in Figure 4 B. The histograms show that the distributions from  
299 the simulations from both models approximate the peak of the distribution of the observations,  
300 however, the simulated concentration distributions have a lower tail that is not seen in the  
301 observed data. This discrepancy could be a product of how the predicted dissolved P  
302 concentration is being calculated in the model (see 3.2.1). The observations reported are  
303 aggregated daily mean values calculated from monitoring observations taken every 10-  
304 minutes. These daily means necessarily do not reflect the full range of concentration variability  
305 in the monitoring data, especially for extreme or short duration hydrological events, and they  
306 do not show diel P variations due to changes in temperature, light, and precipitation (Bieroza  
307 et al., 2023), which are likely to affect P mobilisation, delivery, and in-stream uptake. For  
308 example, see Table 3 for a comparison between the daily mean P and the 10-minutes P  
309 observations. Furthermore, the detection of low P concentrations is restricted by the instrument  
310 detection limits (0.01– 5.00 mg l<sup>-1</sup>). Although neither model reproduces the width of the  
311 observed data distributions, the simulated distributions from Model A are broader than those  
312 from Model B suggesting that Model B is marginally better constrained. Importantly, the  
313 models predict flow-weighted concentrations (normalized by both time and discharge) rather  
314 than time-weighted (mean concentration in stream water as it passes the sampling point), which  
315 could in some cases better represent nutrient concentrations (i.e., for lakes, Rowland et al.,  
316 (2021)). This may result in the different dilution effect in the model compared to the  
317 observations (see mean ( $\mu$ ) total discharge ( $Q$ , m<sup>3</sup>), in Table 4). Monthly density plots show  
318 little to no seasonality, probably masked by model assumptions, which are further discussed in  
319 Table 5. Overall, the model represents the observed distribution between the 25<sup>th</sup> and 75<sup>th</sup>  
320 percentile very well, indicating strong predictive performance. This is especially notable when



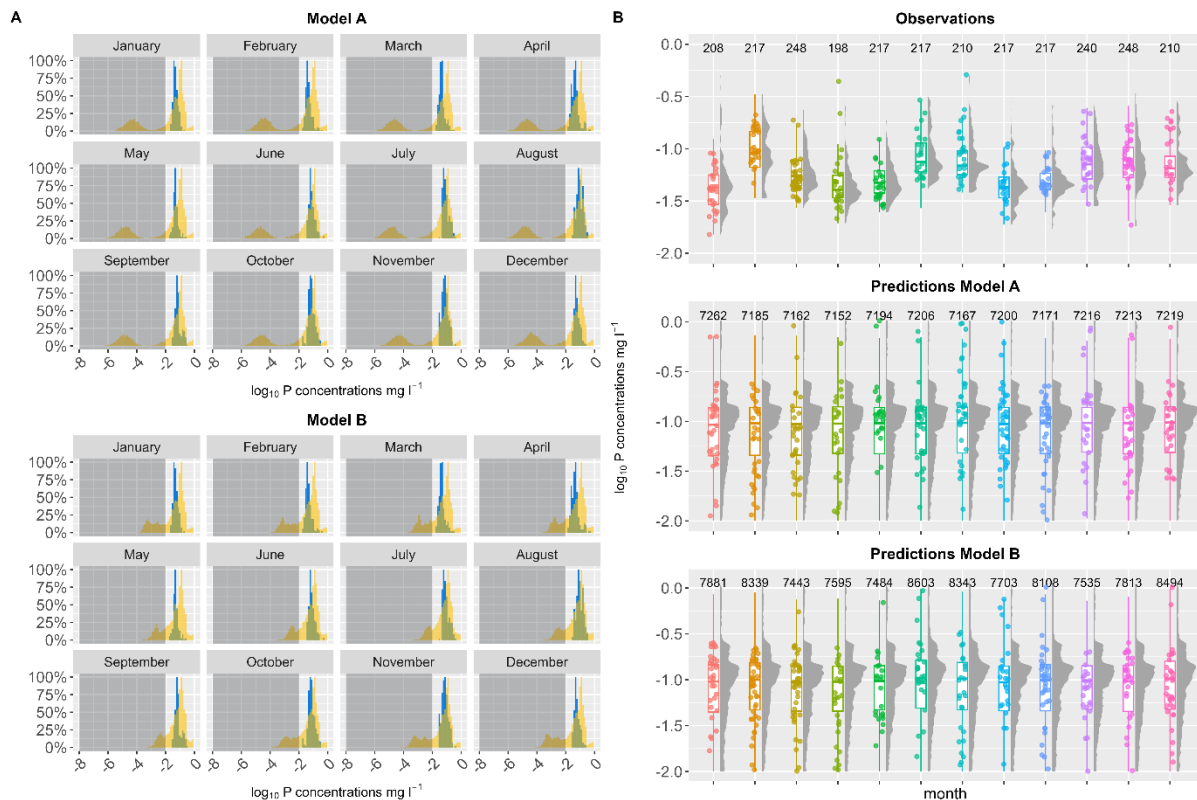
321 considering the small units (P concentrations) that are being reproduced and the complexities  
 322 of processes affecting P dynamics in river catchments.

323

324 *Table 3 Monitored TRP concentrations (mg l<sup>-1</sup>) characteristics (correlation between the two datasets was 0.91). The two*  
 325 *datasets have not been censored with the instrument's detection limits for this analysis, nor log-transformed.*

	10-minute concentration data	Daily mean concentration data
	mg l <sup>-1</sup>	
<b>Min</b>	0.002	0.015
<b>25<sup>th</sup> percentile</b>	0.042	0.043
<b>Median</b>	0.057	0.058
<b>75<sup>th</sup> percentile</b>	0.082	0.085
<b>Mean</b>	0.075	0.075
<b>Max</b>	3.095	1.065

326



327

328 *Figure 4 A represents the histograms of each month's log<sub>10</sub> of TRP concentrations (mg l<sup>-1</sup>), observations are shown in blue,*  
 329 *predictions obtained from the Diffuse P model (Model A, top figure) and Diffuse + Point P model (Model B, bottom figure)*  
 330 *are shown in yellow. The histograms placed outside the grey box show values outside the limit of detection (0.01-5.00 mg l<sup>-1</sup>).*  
 331 *B represents the monthly density plots of log<sub>10</sub> observations (top), the Diffuse P model (middle), and the Diffuse + Point*  
 332 *P model (bottom). Data outside the instrument's limit of detection (0.01-5.00 mg l<sup>-1</sup>) were excluded from the plots in box B,*  
 333 *and the text shows the number of valid samples for each model. The density plots in box B were produced with the ggdist R*  
 334 *package version 3.3.0 (Kay, 2023).*

335

336 Table 4 summarizes each month's characteristics in terms of mean and median P  
337 concentrations, as well as mean discharge and model percentage bias calculated for the two  
338 BBNs. Percentage bias shows that the difference between the two models is minimal,  
339 corroborated by the nearly identical performance in terms of mean predicted concentrations.  
340 Mean total discharge ( $Q$ ,  $m^3$ ) is shown for Model B and the observations, assuming to be the  
341 same for Model A. The ratio between the modelled and the observed discharge shows how the  
342 models simulate 80-100% of flow correctly in most cases, except the summer months, when  
343 the modelled discharge is 60-70% of the observed. This slight underprediction can explain why  
344 the model average concentrations are higher than the observed ones (less discharge, less  
345 dilution).

346

347

348

349

Table 4 Summary of monthly characteristics and results, including model bias. Percentage bias and TRP concentrations have been calculated excluding data outside the instrument's limit of detection (0.01-5.00 mg l<sup>-1</sup>). "A" columns show results for Model A and "B" columns show results for Model B. Both observed and predicted TRP concentrations were log-transformed before calculating the statistics, and then converted back to normal values.

	Percentage bias of simulations against distribution fitted to observed		mean ( $\mu$ ) concentrations			median concentrations			lower limit concentrations ( $\mu-1\sigma$ )			upper limit concentrations ( $\mu+1\sigma$ )			Mean total discharge (Q)		model/ observations ratio
			(mg l <sup>-1</sup> )			(mg l <sup>-1</sup> )			(mg l <sup>-1</sup> )			(mg l <sup>-1</sup> )			m <sup>3</sup>		
	A	B	A	B	obs	A	B	obs	A	B	obs	A	B	obs	Models	obs	
<b>Jan</b>	69.4	74.5	0.08	0.08	0.05	0.09	0.10	0.04	0.03	0.03	0.03	0.20	0.21	0.07	9.99*10 <sup>5</sup>	11.0*10 <sup>5</sup>	0.9
<b>Feb</b>	74.5	70.9	0.08	0.08	0.04	0.09	0.09	0.04	0.03	0.03	0.03	0.21	0.20	0.07	7.42*10 <sup>5</sup>	7.48*10 <sup>5</sup>	1
<b>Mar</b>	67.5	70.7	0.08	0.08	0.04	0.09	0.09	0.04	0.03	0.03	0.03	0.20	0.20	0.07	4.07*10 <sup>5</sup>	4.83*10 <sup>5</sup>	0.8
<b>Apr</b>	69.9	77.9	0.08	0.08	0.05	0.09	0.09	0.04	0.03	0.03	0.03	0.20	0.21	0.09	2.73*10 <sup>5</sup>	3.06*10 <sup>5</sup>	0.9
<b>May</b>	69	81	0.08	0.08	0.05	0.10	0.10	0.05	0.03	0.03	0.02	0.20	0.22	0.07	2.03*10 <sup>5</sup>	2.28*10 <sup>5</sup>	0.9
<b>Jun</b>	73.5	89.2	0.08	0.09	0.07	0.10	0.10	0.07	0.03	0.03	0.03	0.20	0.23	0.13	1.40*10 <sup>5</sup>	2.24*10 <sup>5</sup>	0.6
<b>Jul</b>	70.3	101	0.08	0.09	0.09	0.09	0.10	0.07	0.03	0.03	0.05	0.20	0.24	0.14	0.85*10 <sup>5</sup>	1.15*10 <sup>5</sup>	0.7
<b>Aug</b>	68.5	89.1	0.08	0.09	0.09	0.09	0.10	0.09	0.03	0.03	0.05	0.20	0.23	0.16	1.51*10 <sup>5</sup>	2.52*10 <sup>5</sup>	0.6
<b>Sept</b>	76.5	95.6	0.09	0.09	0.07	0.10	0.10	0.06	0.04	0.03	0.04	0.21	0.24	0.12	1.05*10 <sup>5</sup>	1.03*10 <sup>5</sup>	1
<b>Oct</b>	72.2	73.8	0.08	0.08	0.07	0.10	0.09	0.07	0.03	0.03	0.04	0.2	0.21	0.13	3.94*10 <sup>5</sup>	4.41*10 <sup>5</sup>	0.9
<b>Nov</b>	73.8	71.8	0.09	0.08	0.07	0.10	0.10	0.07	0.03	0.03	0.04	0.21	0.21	0.12	9.10*10 <sup>5</sup>	9.83*10 <sup>5</sup>	0.9
<b>Dec</b>	73.8	72.5	0.08	0.08	0.06	0.09	0.09	0.05	0.03	0.03	0.04	0.20	0.20	0.09	10.10*10 <sup>5</sup>	11.20*10 <sup>5</sup>	0.9

350

### 351 3.2.3 Phosphorus concentrations in the stream – risk of exceeding WFD standards

352 For a speedy evaluation of the P loss risk, in-stream P concentrations were discretized  
353 according to the Environmental Quality Standard (EQS) for both models and evaluated against  
354 similarly discretised lognormal distribution fitted to the observed in-stream TRP. The EQS was  
355 classified as good (between 0 and 0.035 mg l<sup>-1</sup>) and bad (above 0.035 mg l<sup>-1</sup>), as 0.035 mg l<sup>-1</sup>  
356 is the phosphate threshold established in Ireland to comply with the Water Framework  
357 Directive (European Communities Environmental Objectives (Surface Waters) Regulations,  
358 2009). The comparison was done by censoring the concentrations for the instrument's limit of  
359 detection (0.01 – 5.00 mg l<sup>-1</sup>). Overall, both models show a repartition good/bad threshold  
360 close to 40/60 % (data not shown), however, that is lower than the monthly EQS in the  
361 distribution fitted to the observations. The fitted observations agree with Mellander et al.,  
362 (2022), who also showed that the probability of exceeding the EQS in this catchment was  
363 93.7% of the time (data from 2010 to 2020). This discrepancy may be explained by the model's  
364 predicted TRP concentration distribution's inherent shape, which was left-skewed in  
365 comparison to the observational data, and by the censoring process, which might have caused  
366 a shift of the distribution towards 0.01 mg l<sup>-1</sup>.

367

### 368 3.3 Model strengths and limitations

369 We designed a BBN to describe and calculate TRP losses at the catchment outlet in a grassland-  
370 dominated Irish agricultural catchment. As compared to the steady-state probabilistic  
371 conceptual catchment model of P pollution risk by Glendell et al., (2022), the present model  
372 was parameterized using high-resolution datasets, including seven years of daily turbidity  
373 (NTU) and discharge (m<sup>3</sup>) data at the catchment outlet, average soil Morgan P at field scale,  
374 and average measured farmyard size (instead of using a proxy of size). Using high-resolution  
375 turbidity data to calculate sediment losses at catchment outlet simplified the representation of  
376 erosion processes, thus avoiding assumptions regarding erosion rates, delivery, and the

377 contribution of agricultural drains. Furthermore, the model was calibrated using seven years of  
378 daily observed TRP concentrations.

379 Model performance in terms of percentage bias between 76-85% was close to the 50%  
380 acceptable range and appears small, given the small concentration values being simulated.  
381 Additionally, in terms of inter-quantile ranges, this BBN's performance approximates that of  
382 Glendell et al., (2022) BBN in the best performing catchments (Linkwood, Rough, and Lunan  
383 catchments) but is better constrained than the previous study's model in worse performing  
384 catchments.

385 We offer an overview of the model assumption and subsequent potential limitations that we  
386 deem relevant in Table 5, highlighting several research gaps around P modelling in agricultural  
387 catchments. Specifically, there is still uncertainty revolving around point sources, where weak  
388 priors from the literature were introduced due to a lack of monitoring data, as well as a  
389 simplification of soil P sources (Morgan P), which, albeit measured at high resolution, were  
390 represented at discrete levels (indexes) used for monitoring, which may lead to loss of  
391 information. Table 5 also introduces the lack of in-stream biological P uptake, a process that  
392 could be significant in spring and summer, and could improve the model's representation of  
393 reality (Jackson-Blake et al., 2015).

<b>Model assumptions</b>	<b>Consequences</b>
No in-stream removal by biota or sediment absorption.	In-stream P concentrations may be overestimated. However, these processes are secondary, especially considering the extreme flashiness of this catchment.
The main soil P source is spatially available at field resolution; however, the “Morgan P” node was implemented using the categorical classification used in field monitoring.	The categorical variable “Morgan P” can be used for testing management scenarios, however, discretization can lead to loss of information and impact decision making (Landuyt et al., 2013; Nojavan et al., 2017).
Amount of WEP transported to stream “Predicted Dissolved P Concentration” based on the equation for the closed period only, from the 15 <sup>th</sup> of October to the 12 <sup>th</sup> of January, when farmers are forbidden from spreading fertilizer on land in Ireland (Thomas et al., 2016b). The equation is applied to all months, and negative values are substituted with zeroes (see Table 1).	25% of the simulated values of this variable were zeroes, which probably skewed the in-stream concentration posterior distribution as discussed in section 3.2.1. This could be a contributing factor in the masking of seasonality in the model.
Septic tanks modelled as a surface process, although soil risk classes have been included (Glendell et al., 2021), see variable “Soil risk factor” in section 2.4.	Might be underestimating P losses from STs.
P concentrations in septic tanks after primary or secondary treatment are based on (optimistic) Scottish EPA guidelines of Total P concentration reduction (Brownlie et al., 2014) even though the objective of the modelling was TRP.	There is uncertainty surrounding the actual TP/ TRP concentration in a septic tank after primary or secondary treatment, and therefore more data is needed for this model compartment, as well as sensitivity testing.
Septic tanks were assumed to be working, no hypothesis was made regarding failure.	Might be underestimating P losses from STs.
There is no measured data for septic tank P concentration or loads, thus each month the load from septic tanks “Realised total load” is the same, as it is not dependent on discharge (Q).	Septic tank loads are not expected to vary seasonally; therefore, the model could be representing the domestic wastewater systems well, however, this could be one of the factors masking any seasonality in the model. However, septic tank loads have temporal patterns too, and are considered to be an important source of nutrients during spring and summer (Withers et al., 2014).
P concentrations from farmyards are modelled according to literature, however Moloney et al., (2020) found higher concentrations of TP in farmyard drains than that found by Harrison et al., (2019) (about 37 times).	Farmyard losses in the catchment cannot be estimated, and the uncertainty around these losses in the literature is very high, thus the model may be under or overestimating these losses. Further data collection is needed to test these assumptions.
The hydrology compartment, and consequently the rest of the model, was set up at a monthly time step.	This allows the integration of both sparse and high-resolution datasets, as well as the chance for future evaluation of management actions and mitigation measures. This also means that the model does not represent events and hot moments, which usually represent the larger contribution of P losses in a catchment, with climate change expected to <b>increase their contribution</b> (Ockenden et al., 2016).
Both models are calibrated and validated against daily averages of TRP concentration. The daily resolution data may not represent the full variability of the in-stream concentrations (statistics on the two datasets are shown in Table 3).	The model appears to simulate higher TRP concentrations in the upper quartiles than the observations (Table 2), but these may be realistic if compared against the sub-hourly dataset.

395

396 **4. Conclusions**

397 In this study, we combined different methodologies for using high-frequency water quality  
 398 datasets to inform the priors of a BBN aimed at modelling P losses in Irish agricultural  
 399 catchments. Different sources of P were introduced in the modelling exercise in a step-wise

400 fashion, thus improving the model predictive ability and testing the model structural  
401 uncertainty. The two developed BBNs were able to predict the mean and median P  
402 concentrations in the stream well overall, with some limitations apparent in performance at the  
403 monthly time-step. However, the models' predictions presented wider distributions than the  
404 observations, which was noted in a similar work, and remains a property of this stochastic  
405 modelling approach. The BBN modelling approach allowed the inclusion of all the known P  
406 sources in the agricultural catchment, including farmyards, which is rare in P modelling, and  
407 septic tanks, which are often overlooked as P sources. In addition, this study directly reported  
408 on experts' role and selection as an effort to increase transparency. The probabilistic modelling  
409 highlighted the need for further targeted data collection to fill important knowledge gaps, even  
410 in a catchment with state-of-the-art high-resolution and long-term monitoring, such as the one  
411 used in this study. Furthermore, the work informed future research steps, which will include  
412 testing of model transferability, the influence of in-stream P cycling (i.e., estimation of removal  
413 by biota, and/or sediment uptake) on model performance, and understanding of P losses under  
414 future climate change scenarios.

415

## 416 **5. Data and model availability**

417 The datasets, models, code for the analysis and figures are available at  
418 [https://github.com/CamillaNegri/Ballycanew\\_Ptool](https://github.com/CamillaNegri/Ballycanew_Ptool) under the MIT license  
419 (<https://github.com/git/git-scm.com/blob/main/MIT-LICENSE.txt>).

420

## 421 **Bibliography**

- 422 Aguilera, P.A., Fernández, A., Fernández, R., Rumí, R., Salmerón, A., 2011. Bayesian networks in  
423 environmental modelling. *Environ. Model. Softw.* 26, 1376–1388.  
424 <https://doi.org/10.1016/j.envsoft.2011.06.004>  
425 Barton, D.N., Kuikka, S., Varis, O., Uusitalo, L., Henriksen, H.J., Borsuk, M., de la Hera, A.,  
426 Farmani, R., Johnson, S., Linnell, J.D., 2012. Bayesian networks in environmental and

427 resource management. *Integr. Environ. Assess. Manag.* 8, 418–429.  
428 <https://doi.org/10.1002/ieam.1327>

429 BayesFusion, 2019. GeNIe 2.4 [WWW Document]. URL <https://www.bayesfusion.com/> (accessed  
430 5.6.20).

431 Beven, K., 2019. Towards a methodology for testing models as hypotheses in the inexact sciences.  
432 *Proc. R. Soc. Math. Phys. Eng. Sci.* 475, 20180862. <https://doi.org/10.1098/rspa.2018.0862>

433 Bieroza, M., Acharya, S., Benisch, J., ter Borg, R.N., Hallberg, L., Negri, C., Pruitt, A., Pucher, M.,  
434 Saavedra, F., Staniszewska, K., van't Veen, S.G.M., Vincent, A., Winter, C., Basu, N.B.,  
435 Jarvie, H.P., Kirchner, J.W., 2023. Advances in Catchment Science, Hydrochemistry, and  
436 Aquatic Ecology Enabled by High-Frequency Water Quality Measurements. *Environ. Sci.*  
437 *Technol.* <https://doi.org/10.1021/acs.est.2c07798>

438 Blöschl, G., Bierkens, M.F.P., Chambel, A., 2019. Twenty-three unsolved problems in hydrology  
439 (UPH) – a community perspective. *Hydrol. Sci. J.* 64, 1141–1158.  
440 <https://doi.org/10.1080/02626667.2019.1620507>

441 Bol, R., Gruau, G., Mellander, P.-E., Dupas, R., Bechmann, M., Skarbøvik, E., Bieroza, M., Djodjic,  
442 F., Glendell, M., Jordan, P., Van der Grift, B., Rode, M., Smolders, E., Verbeeck, M., Gu, S.,  
443 Klumpp, E., Pohle, I., Fresne, M., Gascuel-Oudou, C., 2018. Challenges of Reducing  
444 Phosphorus Based Water Eutrophication in the Agricultural Landscapes of Northwest Europe.  
445 *Front. Mar. Sci.* 5.

446 Borsuk, M.E., Stow, C.A., Reckhow, K.H., 2004. A Bayesian network of eutrophication models for  
447 synthesis, prediction, and uncertainty analysis. *Ecol. Model.* 173, 219–239.  
448 <https://doi.org/10.1016/j.ecolmodel.2003.08.020>

449 Brabec, Macháč, Jílková, 2019. Using Bayesian Networks to Assess Effectiveness of Phosphorus  
450 Abatement Measures under the Water Framework Directive. *Water* 11, 1791.  
451 <https://doi.org/10.3390/w11091791>

452 Brazier, R.E., Heathwaite, A.L., Liu, S., 2005. Scaling issues relating to phosphorus transfer from  
453 land to water in agricultural catchments. *J. Hydrol., Nutrient Mobility within River Basins: A*  
454 *European Perspective* 304, 330–342. <https://doi.org/10.1016/j.jhydrol.2004.07.047>

455 Brownlie, W., May, L., McDonald, C., Roaf, S., Spears, B.M., 2014. Assessment of a novel  
456 development policy for the control of phosphorus losses from private sewage systems to the  
457 Loch Leven catchment, Scotland, UK. *Environ. Sci. Policy* 38, 207–216.  
458 <https://doi.org/10.1016/j.envsci.2013.12.006>

459 Campbell, J.M., Jordan, P., Arnscheidt, J., 2015. Using high-resolution phosphorus data to investigate  
460 mitigation measures in headwater river catchments. *Hydrol. Earth Syst. Sci.* 19, 453–464.  
461 <https://doi.org/10.5194/hess-19-453-2015>

462 Crockford, L., O’Riordain, S., Taylor, D., Melland, A., Shortle, G., Jordan, P., 2017. The application  
463 of high temporal resolution data in river catchment modelling and management strategies.  
464 *Environ. Monit. Assess.* 189, 461. <https://doi.org/10.1007/s10661-017-6174-1>

465 Delignette-Muller, M.-L., Dutang, C., Pouillot, R., Denis, J.-B., Siberchiot, A., 2020. Package  
466 ‘fitdistrplus’: Help to Fit of a Parametric Distribution to Non-Censored or Censored Data.

467 Djodjic, F., Markensten, H., 2019. From single fields to river basins: Identification of critical source  
468 areas for erosion and phosphorus losses at high resolution. *Ambio* 48, 1129–1142.  
469 <https://doi.org/10.1007/s13280-018-1134-8>

470 Environmental Protection Agency Ireland (EPA), 2015. National Inspection Plan: Domestic Waste  
471 Water Treatment Systems: Inspection Data Report 1st July 2013 – 31st December 2014 (No.  
472 ISBN 978-1-84095-615-3). Johnstown Castle, Co. Wexford.

473 Environmental Protection Agency Ireland (EPA), 2003. A catchment based approach for reducing  
474 nutrient inputs from all sources to the lakes of Kilarney: final report. Lough Leane catchment  
475 monitoring and management system. Kerry County Council, Ireland.

476 Environmental Protection Agency Ireland (EPA), 2000. Code of Practice: Wastewater Treatment  
477 Systems for Single Houses.

478 European Communities Environmental Objectives (Surface Waters) Regulations, 2009. S.I. No. 272  
479 of 2009, Dublin: Stationery Office.

480 European Environment Agency, 2019. The European environment: state and outlook 2020 :  
481 knowledge for transition to a sustainable Europe. Publications Office, LU.



482 Evans, D.M., Schoenholtz, S.H., Wigington, P.J., Griffith, S.M., Floyd, W.C., 2014. Spatial and  
483 temporal patterns of dissolved nitrogen and phosphorus in surface waters of a multi-land use  
484 basin. *Environ. Monit. Assess.* 186, 873–887. <https://doi.org/10.1007/s10661-013-3428-4>  
485 Forio, M.A.E., Landuyt, D., Bennetsen, E., Lock, K., Nguyen, T.H.T., Ambarita, M.N.D., Musonge,  
486 P.L.S., Boets, P., Everaert, G., Dominguez-Granda, L., Goethals, P.L.M., 2015. Bayesian  
487 belief network models to analyse and predict ecological water quality in rivers. *Ecol. Model.*  
488 312, 222–238. <https://doi.org/10.1016/j.ecolmodel.2015.05.025>  
489 Gill, L., Ireland, Environmental Protection Agency, Environmental Research Technological  
490 Development and Innovation Programme, 2005. Water framework directive: an investigation  
491 into the performance of subsoils and stratified sand filters for the treatment of wastewater  
492 from on-site systems (2001-MS-15-M1) : synthesis report. Environmental Protection Agency,  
493 Johnstown Castle, Co. Wexford.  
494 Gill, L.W., Mockler, E.M., 2016. Modeling the pathways and attenuation of nutrients from domestic  
495 wastewater treatment systems at a catchment scale. *Environ. Model. Softw.* 84, 363–377.  
496 <https://doi.org/10.1016/j.envsoft.2016.07.006>  
497 Gill, L.W., O’Súilleabháin, C., Misstear, B.D.R., Johnston, P.J., 2007. The Treatment Performance of  
498 Different Subsoils in Ireland Receiving On-Site Wastewater Effluent. *J. Environ. Qual.* 36,  
499 1843–1855. <https://doi.org/10.2134/jeq2007.0064>  
500 Glendell, M., Gagkas, Z., Richards, S., Halliday, S., 2021. Developing a probabilistic model to  
501 estimate phosphorus, nitrogen and microbial pollution to water from septic tanks. Scotland’s  
502 Centre of Expertise for Waters (CREW).  
503 Glendell, M., Gagkas, Z., Stutter, M., Richards, S., Lilly, A., Vinten, A., Coull, M., 2022. A systems  
504 approach to modelling phosphorus pollution risk in Scottish rivers using a spatial Bayesian  
505 Belief Network helps targeting effective mitigation measures. *Front. Environ. Sci.* 10.  
506 Glendell, M., Palarea-Albaladejo, J., Pohle, I., Marrero, S., McCreadie, B., Cameron, G., Stutter, M.,  
507 2019. Modeling the Ecological Impact of Phosphorus in Catchments with Multiple  
508 Environmental Stressors. *J. Environ. Qual.* 48, 1336–1346.  
509 <https://doi.org/10.2134/jeq2019.05.0195>  
510 Harris, G.P., Heathwaite, A.L., 2012. Why is achieving good ecological outcomes in rivers so  
511 difficult? *Freshw. Biol.* 57, 91–107. <https://doi.org/10.1111/j.1365-2427.2011.02640.x>  
512 Harrison, S., McAree, C., Mulville, W., Sullivan, T., 2019. The problem of agricultural ‘diffuse’  
513 pollution: Getting to the point. *Sci. Total Environ.* 677, 700–717.  
514 <https://doi.org/10.1016/j.scitotenv.2019.04.169>  
515 Haygarth, P.M., Condrón, L.M., Heathwaite, A.L., Turner, B.L., Harris, G.P., 2005. The phosphorus  
516 transfer continuum: Linking source to impact with an interdisciplinary and multi-scaled  
517 approach. *Sci. Total Environ.* 344, 5–14. <https://doi.org/10.1016/j.scitotenv.2005.02.001>  
518 Jackson-Blake, L., Wade, A., Futter, M., Butterfield, D., Couture, R.-M., Cox, B., Crossman, J.,  
519 Ekholm, P., Halliday, S., Jin, L., Lawrence, D.S.L., Lepistö, A., Lin, Y., Rankinen, K.,  
520 Whitehead, P., 2016. The INTEgrated CATCHment model of phosphorus dynamics (INCA-P):  
521 Description and demonstration of new model structure and equations. *Environ. Model. Softw.*  
522 83, 356–386. <https://doi.org/10.1016/j.envsoft.2016.05.022>  
523 Jackson-Blake, L.A., Dunn, S.M., Helliwell, R.C., Skeffington, R.A., Stutter, M.I., Wade, A.J., 2015.  
524 How well can we model stream phosphorus concentrations in agricultural catchments?  
525 *Environ. Model. Softw.* 64, 31–46. <https://doi.org/10.1016/j.envsoft.2014.11.002>  
526 Jackson-Blake, L.A., Sample, J.E., Wade, A.J., Helliwell, R.C., Skeffington, R.A., 2017. Are our  
527 dynamic water quality models too complex? A comparison of a new parsimonious  
528 phosphorus model, SimplyP, and INCA-P: OVER-COMPLEXITY IN WATER QUALITY  
529 MODELS. *Water Resour. Res.* 53, 5382–5399. <https://doi.org/10.1002/2016WR020132>  
530 Jarvie, H.P., Sharpley, A.N., Flaten, D., Kleinman, P.J.A., 2019. Phosphorus mirabilis: Illuminating  
531 the Past and Future of Phosphorus Stewardship. *J. Environ. Qual.* 48, 1127–1132.  
532 <https://doi.org/10.2134/jeq2019.07.0266>  
533 Jordan, P., Arnscheidt, A., McGrogan, H., McCormick, S., 2007. Characterising phosphorus transfers  
534 in rural catchments using a continuous bank-side analyser. *Hydrol. Earth Syst. Sci.* 11, 372–  
535 381. <https://doi.org/10.5194/hess-11-372-2007>

536 Kaikkonen, L., Parviainen, T., Rahikainen, M., Uusitalo, L., Lehikoinen, A., 2021. Bayesian  
537 Networks in Environmental Risk Assessment: A Review. *Integr. Environ. Assess. Manag.* 17,  
538 62–78. <https://doi.org/10.1002/ieam.4332>

539 Kay, M., 2023. {ggdist}: Visualizations of Distributions and Uncertainty.

540 Kragt, M.E., 2009. A beginners guide to Bayesian network modelling for integrated catchment  
541 management, Landscape Logic Technical Report No. 9.

542 Landuyt, D., Broekx, S., D’hondt, R., Engelen, G., Aertsens, J., Goethals, P.L.M., 2013. A review of  
543 Bayesian belief networks in ecosystem service modelling. *Environ. Model. Softw.* 46, 1–11.  
544 <https://doi.org/10.1016/j.envsoft.2013.03.011>

545 Mellander, P.-E., Galloway, J., Hawtree, D., 2022. Phosphorus mobilization and delivery estimated  
546 from long-term high frequency water quality and discharge data. *Front. Water* 4.  
547 <https://doi.org/10.3389/frwa.2022.917813>

548 Mellander, P.-E., Jordan, P., Bechmann, M., Fovet, O., Shore, M.M., McDonald, N.T., Gascuel-  
549 Odoux, C., 2018. Integrated climate-chemical indicators of diffuse pollution from land to  
550 water. *Sci. Rep.* 8, 1–10. <https://doi.org/10.1038/s41598-018-19143-1>

551 Mellander, P.-E., Jordan, P., Shore, M., Melland, A.R., Shortle, G., 2015. Flow paths and phosphorus  
552 transfer pathways in two agricultural streams with contrasting flow controls. *Hydrol. Process.*  
553 29, 3504–3518. <https://doi.org/10.1002/hyp.10415>

554 Mellander, P.-E., Melland, A.R., Jordan, P., Wall, D.P., Murphy, P.N.C., Shortle, G., 2012.  
555 Quantifying nutrient transfer pathways in agricultural catchments using high temporal  
556 resolution data. *Environ. Sci. Policy, CATCHMENT SCIENCE AND POLICY*  
557 *EVALUATION FOR AGRICULTURE AND WATER QUALITY* 24, 44–57.  
558 <https://doi.org/10.1016/j.envsci.2012.06.004>

559 Mockler, E.M., Deakin, J., Archbold, M., Daly, D., Bruen, M., 2016. Nutrient load apportionment to  
560 support the identification of appropriate water framework directive measures. *Biol. Environ.*  
561 *Proc. R. Ir. Acad.* 116B, 245–263. <https://doi.org/10.3318/bioe.2016.22>

562 Mockler, E.M., Deakin, J., Archbold, M., Gill, L., Daly, D., Bruen, M., 2017. Sources of nitrogen and  
563 phosphorus emissions to Irish rivers and coastal waters: Estimates from a nutrient load  
564 apportionment framework. *Sci. Total Environ.* 601–602, 326–339.  
565 <https://doi.org/10.1016/j.scitotenv.2017.05.186>

566 Moe, S.J., Carriger, J.F., Glendell, M., 2021. Increased Use of Bayesian Network Models Has  
567 Improved Environmental Risk Assessments. *Integr. Environ. Assess. Manag.* 17, 53–61.  
568 <https://doi.org/10.1002/ieam.4369>

569 Moloney, T., Fenton, O., Daly, K., 2020. Ranking connectivity risk for phosphorus loss along  
570 agricultural drainage ditches. *Sci. Total Environ.* 703, 134556.  
571 <https://doi.org/10.1016/j.scitotenv.2019.134556>

572 Nojavan, F., Qian, S.S., Stow, C.A., 2017. Comparative analysis of discretization methods in  
573 Bayesian networks. *Environ. Model. Softw.* 87, 64–71.  
574 <https://doi.org/10.1016/j.envsoft.2016.10.007>

575 Oakley, J., 2020. SHELF: Tools to Support the Sheffield Elicitation Framework.

576 Ockenden, M.C., Deasy, C.E., Benskin, C.McW.H., Beven, K.J., Burke, S., Collins, A.L., Evans, R.,  
577 Falloon, P.D., Forber, K.J., Hiscock, K.M., Hollaway, M.J., Kahana, R., Macleod, C.J.A.,  
578 Reaney, S.M., Snell, M.A., Villamizar, M.L., Wearing, C., Withers, P.J.A., Zhou, J.G.,  
579 Haygarth, P.M., 2016. Changing climate and nutrient transfers: Evidence from high temporal  
580 resolution concentration-flow dynamics in headwater catchments. *Sci. Total Environ.* 548–  
581 549, 325–339. <https://doi.org/10.1016/j.scitotenv.2015.12.086>

582 Packham, I., Mockler, E., Archbold, M., Mannix, A., Daly, D., Deakin, J., Bruen, M., 2020.  
583 Catchment Characterisation Tool: Prioritising Critical Source Areas for managing diffuse  
584 nitrate pollution. *Environ. Model. Assess.* 25, 23–39. <https://doi.org/10.1007/s10666-019-09683-9>

586 Pappenberger, F., Beven, K.J., 2006. Ignorance is bliss: Or seven reasons not to use uncertainty  
587 analysis. *Water Resour. Res.* 42. <https://doi.org/10.1029/2005WR004820>

588 Penk, M.R., Bruen, M., Feld, C.K., Piggott, J.J., Christie, M., Bullock, C., Kelly-Quinn, M., 2022.  
589 Using weighted expert judgement and nonlinear data analysis to improve Bayesian belief

590 network models for riverine ecosystem services. *Sci. Total Environ.* 851, 158065.  
591 <https://doi.org/10.1016/j.scitotenv.2022.158065>

592 Phan, T.D., Smart, J.C.R., Stewart-Koster, B., Sahin, O., Hadwen, W.L., Dinh, L.T., Tahmasbian, I.,  
593 Capon, S.J., 2019. Applications of Bayesian Networks as Decision Support Tools for Water  
594 Resource Management under Climate Change and Socio-Economic Stressors: A Critical  
595 Appraisal. *Water* 11, 2642. <https://doi.org/10.3390/w11122642>

596 Radcliffe, D.E., Freer, J., Schoumans, O., 2009. Diffuse phosphorus models in the United States and  
597 Europe: their usages, scales, and uncertainties. *J. Environ. Qual.* 38, 1956–1967.  
598 <https://doi.org/10.2134/jeq2008.0060>

599 Regan, J., Fenton, O., Healy, M., 2012. A Review of Phosphorus and Sediment Release from Irish  
600 Tillage Soils, the Methods Used to Quantify Losses and the Current State of Mitigation  
601 Practice. *Biol. Environ. Proc. R. Ir. Acad.* 112, 157–183.  
602 <https://doi.org/10.3318/BIOE.2012.05>

603 Rode, M., Arhonditsis, G., Balin, D., Kebede, T., Krysanova, V., Griensven, A. van, Zee, S.E.A.T.M.  
604 van der, 2010. New challenges in integrated water quality modelling. *Hydrol. Process.* 24,  
605 3447–3461. <https://doi.org/10.1002/hyp.7766>

606 Rowland, F.E., Stow, C.A., Johnson, L.T., Hirsch, R.M., 2021. Lake Erie tributary nutrient trend  
607 evaluation: Normalizing concentrations and loads to reduce flow variability. *Ecol. Indic.* 125,  
608 107601. <https://doi.org/10.1016/j.ecolind.2021.107601>

609 Sahlin, U., Helle, I., Perepolkin, D., 2021. “This Is What We Don’t Know”: Treating Epistemic  
610 Uncertainty in Bayesian Networks for Risk Assessment. *Integr. Environ. Assess. Manag.* 17,  
611 221–232. <https://doi.org/10.1002/ieam.4367>

612 Schulte, R.P.O., Melland, A.R., Fenton, O., Herlihy, M., Richards, K., Jordan, P., 2010. Modelling  
613 soil phosphorus decline: Expectations of Water Framework Directive policies. *Environ. Sci.*  
614 *Policy* 13, 472–484. <https://doi.org/10.1016/j.envsci.2010.06.002>

615 Sherriff, S., Rowan, J.S., Melland, A.R., Jordan, P., Fenton, O., Ó hUallacháin, D., 2015.  
616 Investigating suspended sediment dynamics in contrasting agricultural catchments using ex  
617 situ turbidity-based suspended sediment monitoring. *Hydrol. Earth Syst. Sci.* 19, 3349–3363.  
618 <https://doi.org/10.5194/hess-19-3349-2015>

619 Shore, M., Jordan, P., Mellander, P.-E., Kelly-Quinn, M., Daly, K., Sims, J.T., Wall, D.P., Melland,  
620 A.R., 2016. Characterisation of agricultural drainage ditch sediments along the phosphorus  
621 transfer continuum in two contrasting headwater catchments. *J. Soils Sediments* 16, 1643–  
622 1654. <https://doi.org/10.1007/s11368-015-1330-0>

623 Shore, M., Jordan, P., Mellander, P.-E., Kelly-Quinn, M., Melland, A.R., 2015. An agricultural  
624 drainage channel classification system for phosphorus management. *Agric. Ecosyst. Environ.*  
625 199, 207–215. <https://doi.org/10.1016/j.agee.2014.09.003>

626 Shore, M., Jordan, P., Mellander, P.-E., Kelly-Quinn, M., Wall, D.P., Murphy, P.N.C., Melland, A.R.,  
627 2014. Evaluating the critical source area concept of phosphorus loss from soils to water-  
628 bodies in agricultural catchments. *Sci. Total Environ.* 490, 405–415.  
629 <https://doi.org/10.1016/j.scitotenv.2014.04.122>

630 Stutter, M., Barros Costa, F., O Huallachain, D., 2021. Riparian buffer zone quantitative effectiveness  
631 review database 3. <https://doi.org/10.17632/t64dbpv63x.3>

632 Teagasc - Agriculture and Food Development Authority, 2018. Agricultural Catchments Programme -  
633 Phase 2 Report.

634 Thomas, I.A., Bruen, M., Mockler, E., Werner, C., Mellander, P.-E., Reaney, S., Rymaszewicz, A.,  
635 McGrath, G., Eder, E., Wade, A.J., Collins, A., Arheimer, B., 2021. Catchment Models and  
636 Management Tools for Diffuse Contaminants (Sediment, Phosphorus and Pesticides):  
637 DiffuseTools Project (No. 396). ENVIRONMENTAL PROTECTION AGENCY An  
638 Ghníomhaireacht um Chaomhnú Comhshaoil PO Box 3000, Johnstown Castle, Co. Wexford,  
639 Ireland.

640 Thomas, I.A., Jordan, P., Mellander, P.-E., Fenton, O., Shine, O., Ó hUallacháin, D., Creamer, R.,  
641 McDonald, N.T., Dunlop, P., Murphy, P.N.C., 2016a. Improving the identification of  
642 hydrologically sensitive areas using LiDAR DEMs for the delineation and mitigation of  
643 critical source areas of diffuse pollution. *Sci. Total Environ.* 556, 276–290.  
644 <https://doi.org/10.1016/j.scitotenv.2016.02.183>

- 645 Thomas, I.A., Mellander, P.-E., Murphy, P.N.C., Fenton, O., Shine, O., Djodjic, F., Dunlop, P.,  
646 Jordan, P., 2016b. A sub-field scale critical source area index for legacy phosphorus  
647 management using high resolution data. *Agric. Ecosyst. Environ.* 233, 238–252.  
648 <https://doi.org/10.1016/j.agee.2016.09.012>
- 649 Uusitalo, L., 2007. Advantages and challenges of Bayesian networks in environmental modelling.  
650 *Ecol. Model.* 203, 312–318. <https://doi.org/10.1016/j.ecolmodel.2006.11.033>
- 651 Vero, S.E., Daly, K., McDonald, N.T., Leach, S., Sherriff, S., Mellander, P.-E., 2019. Sources and  
652 Mechanisms of Low-Flow River Phosphorus Elevations: A Repeated Synoptic Survey  
653 Approach. *Water* 11, 1497. <https://doi.org/10.3390/w11071497>
- 654 Wade, A.J., Jackson, B.M., Butterfield, D., 2008. Over-parameterised, uncertain ‘mathematical  
655 marionettes’ — How can we best use catchment water quality models? An example of an 80-  
656 year catchment-scale nutrient balance. *Sci. Total Environ.* 400, 52–74.  
657 <https://doi.org/10.1016/j.scitotenv.2008.04.030>
- 658 Wall, D., Jordan, P., Melland, A.R., Mellander, P.-E., Buckley, C., Reaney, S.M., Shortle, G., 2011.  
659 Using the nutrient transfer continuum concept to evaluate the European Union Nitrates  
660 Directive National Action Programme. *Environ. Sci. Policy* 14, 664–674.  
661 <https://doi.org/10.1016/j.envsci.2011.05.003>
- 662 Wall, D.P., Murphy, P.N.C., Melland, A.R., Mehan, S., Shine, O., Buckley, C., Mellander, P.-E.,  
663 Shortle, G., Jordan, P., 2012. Evaluating nutrient source regulations at different scales in five  
664 agricultural catchments. *Environ. Sci. Policy* 24, 34–43.  
665 <https://doi.org/10.1016/j.envsci.2012.06.007>
- 666 Wellen, C., Kamran-Disfani, A.-R., Arhonditsis, G.B., 2015. Evaluation of the Current State of  
667 Distributed Watershed Nutrient Water Quality Modeling. *Environ. Sci. Technol.* 49, 3278–  
668 3290. <https://doi.org/10.1021/es5049557>
- 669 Withers, P.J., Jordan, P., May, L., Jarvie, H.P., Deal, N.E., 2014. Do septic tank systems pose a  
670 hidden threat to water quality? *Front. Ecol. Environ.* 12, 123–130.  
671 <https://doi.org/10.1890/130131>
- 672 Zambrano-Bigiarini, M., 2020. hydroGOF: Goodness-of-Fit Functions for Comparison of Simulated  
673 and Observed Hydrological Time Series. <https://doi.org/10.5281/zenodo.839854>
- 674

675 **Acknowledgements:** We acknowledge the Teagasc Walsh Scholar Programme for providing  
676 the funding (Reference Number 2019021). We thank the experts for providing support in the  
677 model development as well as useful insights and directions, as well as the referees without  
678 whom the final draft of this paper would not have been possible. Last but not least, we wish to  
679 thank Orla Shortall, Evangelia Apostolakopoulou, and the whole the Research Ethics  
680 Committee at The James Hutton Institute; Edward Burgess, Mark Boland, Bridget Lynch, Una  
681 Cullen, and Simon Leach at the Teagasc Agricultural Catchments Programme for providing  
682 and explaining datasets, as well as giving context and insights on the catchments.

683

684 **Conflict of interest** The Authors declare no conflict of interest.

## 685 **Figure captions**

686 Figure 1 Study area: the Ballycanew catchment in County Wexford. Elevation varies between 21 m  
687 a.s.l. and 232 m a.s.l. The location of the hydrometric station is marked with the black dot, while  
688 magenta lines represent streams and yellow lines represent artificial drainage.

689 Figure 2 Structure of the final BBNs, including the additional nodes for Model B highlighted inside  
690 the box.

691 Figure 3 Overall distribution density of log<sub>10</sub> TRP concentrations fitted to observations versus those  
692 predicted by the two developed BBNs. BBN predictions show a larger variance, the full extent of  
693 which is shown in the plot by the density and box plots and scattered data points. Data outside the  
694 instrument's limit of detection (0.01-5.00 mg l<sup>-1</sup>) were excluded from the plot, and the text shows the  
695 number of valid samples for each model. This plot was produced with the ggdist R package version  
696 3.3.0 (Kay, 2023).

697 Figure 4 A represents the histograms of each month's log<sub>10</sub> of TRP concentrations (mg L<sup>-1</sup>),  
698 observations are shown in blue, predictions obtained from the Diffuse P model (Model A, top figure)  
699 and Diffuse + Point P model (Model B, bottom figure) are shown in yellow. The histograms placed  
700 outside the grey box show values outside the limit of detection (0.01-5.00 mg l<sup>-1</sup>). B represents the  
701 monthly density plots of log<sub>10</sub> observations (top), the Diffuse P model (middle), and the Diffuse +  
702 Point P model (bottom). Data outside the instrument's limit of detection (0.01-5.00 mg l<sup>-1</sup>) were  
703 excluded from the plots in box B, and the text shows the number of valid samples for each model. The  
704 density plots in box B were produced with the ggdist R package version 3.3.0 (Kay, 2023).

705

## 706 **Table captions**

707 Table 1 Model specifications organized by sub-model. The "Hydrology, "Management", and  
708 "Erosion" sub-models belong to both Model A and B.

709 Table 2 The two model's overall performances in terms of mean, standard deviation, quantiles, and  
710 percentage bias. Data outside the instrument's limit of detection (0.01-5.00 mg l<sup>-1</sup>) were excluded  
711 from the calculations. Both observed and predicted TRP concentrations were log-transformed before  
712 calculating the statistics, and then converted back to normal values.

713 Table 3 Monitored TRP concentrations (mg l<sup>-1</sup>) characteristics (correlation between the two datasets  
714 was 0.91). The two datasets have not been censored with the instrument's detection limits for this  
715 analysis, nor log-transformed.

716 Table 4 Summary of monthly characteristics and results, including model bias. Percentage bias and  
717 TRP concentrations have been calculated excluding data outside the instrument's limit of detection  
718 (0.01-5.00 mg l<sup>-1</sup>). "A" columns show results for Model A and "B" columns show results for Model  
719 B. Both observed and predicted TRP concentrations were log-transformed before calculating the  
720 statistics, and then converted back to normal values.

721 Table 5 Model assumptions, limitations, and strengths

722

723 **Appendix A: catchment characteristics**

			<b>Reference</b>
<b>General</b>	<b>Location</b>	52°36'N, 6°20'W	Sherriff et al., (2015)
	<b>Size</b>	1191 ha	Teagasc - Agriculture and Food Development Authority, (2018)
	<b>Median slope</b>	3°	Sherriff et al., (2015)
	<b>Altitude (m a.s.l.)</b>	40-200	Mellander et al., (2015)
	<b>Average field size (ha)</b>	3.04	Thomas et al., (2016b)
<b>Management</b>	<b>Land use</b>	78% grassland, 20% tillage	Teagasc - Agriculture and Food Development Authority, (2018)
	<b>Stocking rate (LU ha<sup>-1</sup>)</b>	1.04	Sherriff et al., (2015)
<b>Hydrology</b>	<b>Soil series</b>	Typical Surface-water, Gleys or Groundwater, Gleys (71%), Typical Brown Earths (29%)	Thomas et al., (2016a)
	<b>Drainage class</b>	Poorly drained, well-drained in the uplands	Teagasc - Agriculture and Food Development Authority, (2018)
	<b>Proportion of poorly drained soils on total area</b>	85%	Shore et al., (2014)
	<b>Dominant flow pathway</b>	Surface	Thomas et al., (2016a)
	<b>Stream order</b>	2	Mellander et al., (2012)
	<b>Runoff coefficient 2009-2014</b>	0.48	Thomas et al., (2016b)
	<b>Runoff flashiness (Q5:Q95)</b>	202	Thomas et al., (2016b)
	<b>Runoff Flashiness 2010-2020 (Q5/Q95)</b>	126	Mellander et al., (2022)
	<b>Ditch density (km<sup>2</sup>km<sup>-2</sup>) and area of channel network (% of catchment area)</b>	1.3 (1.26%)	Shore et al., (2015)
	<b>Channel density (%) per sediment retention class</b>	Low (15%), low-moderate (10%), moderate-high (26%), high (49%)	Shore et al., (2015)
	<b>Annual discharge 2010-2020 (mm yr<sup>-1</sup>)</b>	1051	Mellander et al., (2022)
<b>P loss</b>	<b>Mean suspended sediment concentrations 2009-2012 (mg l<sup>-1</sup>)</b>	14	Sherriff et al., (2015)
	<b>Mean suspended solids loads 2009-2012 (t km<sup>-2</sup>yr<sup>-1</sup>)</b>	26.64	Sherriff et al., (2015)
	<b>Average P losses (kg TP ha<sup>-1</sup>) 2010-2013</b>	1.035	Mellander et al., (2015)
	<b>Total Dissolved P (mg l<sup>-1</sup>) ~ Total Reactive P (mg l<sup>-1</sup>) at catchment outlet</b>	TDP = 1.1475*TRP + 0.0078	Shore et al., (2014)
	<b>% areas at highest risk of legacy soil P transfers in baseline and (resampled) years with CSA Index threshold ≥ 5</b>	5.6 (4.1)	(Thomas et al., (2016b)
	<b>Water Extractable P (WEP) ~ Soil Morgan P</b>	WEP = 0.58*SoilMorganP+1.13	Thomas et al., (2016b)
<b>Connectivity</b>	<b>Mean HSA size m<sup>2</sup> (% of catchment)<sup>b</sup></b>	703147 (6)	Thomas et al., (2016a)
	<b>% hydrologically disconnected area over total catchment area<sup>c</sup></b>	24.9	Thomas et al., (2016a)

724

725

726 **Authors contributions**

727 **Camilla Negri** Conceptualization, Methodology, Formal analysis, Data Curation, Writing -  
728 Original Draft, Visualization, Writing - Review & Editing. **Per-Erik Mellander:**  
729 Conceptualization, Funding acquisition, Data Curation, Writing - Review & Editing,  
730 Supervision. **Nicholas Schurch:** Conceptualization, Methodology, Writing - Review &  
731 Editing, Supervision. **Andrew J. Wade:** Conceptualization, Funding acquisition, Writing -  
732 Review & Editing, Supervision. **Zisis Gagkas:** Methodology, **Douglas H. Wardell-Johnson:**  
733 Formal analysis, **Kerr Adams:** Methodology, **Miriam Glendell:** Conceptualization, Funding  
734 acquisition, Methodology, Writing - Review & Editing, Resources, Project Administration,  
735 Supervision.

736